Physics – Uspekhi **47** (4) 341 – 358 (2004)

REVIEWS OF TOPICAL PROBLEMS PACS numbers: **25.20.–x**, **41.50.+h**, 41.60.Cr

Photonuclear experiments with Compton-backscattered gamma beams

V G Nedorezov, A A Turinge, Yu M Shatunov

DOI: 10.1070/PU2004v047n04ABEH001743

Contents

Abstract. Experimental research on photonuclear reactions with gamma beams of intermediate energy (from the meson photoproduction threshold up to several GeV) produced by laser photons Compton backscattered on electrons (positrons) circulating in storage rings is reviewed. Common to all of the studies are the subject (interaction mechanisms of gamma-quanta with nuclei) and the experimental technique (Compton beams), which has come to be widely used in recent years. The experimental and applied possibilities offered by the high-intensity Compton beams created in recent years are also discussed.

1. Introduction

The use of gamma-quanta of intermediate energies with wavelengths comparable to the size of a nucleon represents a simple and effective method for investigating nuclear structure at the level of nucleonic and mesonic degrees of freedom. This is because the operator of electromagnetic interaction is quite well studied and photons freely penetrate the nucleus and effectively interact with nucleons. The angular momentum that is then transferred to the nucleus is minimal compared with the case of strongly interacting particles, and the multiplicity of reaction products is relatively small. Therefore, the cross sections of photonuclear reactions clearly exhibit a resonant structure due to the excitation and decay of nucleonic resonances.

In recent years, the main factor confining photonuclear studies to the energy range indicated has been the absence of photon beams with the required parameters, namely, with high intensity, monochromaticity, a high level of polarization, continuity, and low background. Bremsstrahlung beams, which for a long time served as the main instrument in such studies, were not consistent with these requirements, with the exception of intensity. Various methods have been used to improve the beam quality. Most commonly applied has been the method of tagging Bremsstrahlung photons, based on measuring coincidences of electrons scattered on the Bremsstrahlung radiator with the nuclear reaction products. This method has allowed obtaining highly monochromatic beams. Methods were also developed for obtaining polarized Bremsstrahlung photons. At present, successful work with Bremsstrahlung beams is under way at various scientific centers in Europe, the USA, Canada, Japan, and other countries.

The present review deals with the method of Compton backscattering, which has provided additional advantages for investigating photonuclear reactions: a higher degree of beam polarization and a low background. A detailed comparison of various methods of producing gamma-beams can be found in monograph [1]. The present review mainly reflects informa-

V G Nedorezov Institute for Nuclear Research,
Russian Academy of Sciences,
prosp. 60-letiya Oktyabrya 7a, 117312 Moscow, Russian Federation
Tel. (7-095) 135 05 78
E-mail: vladimir@cpc.inr.ac.ru
A A Turinge Russian Research Center 'Kurchatov Institute',
Kurchatov Center for Synchrotron Radiation,
pl. Kurchatova 1, 123182 Moscow, Russian Federation
Tel./Fax (7-095) 196 77 45
E-mail: andrey@cpc.inr.ac.ru
Yu M Shatunov G I Budker Institute of Nuclear Physics,
Siberian Branch of the Russian Academy of Sciences,
prosp. akad. Lavrent'eva 11, 630090 Novosibirsk, Russian Federation
Tel. (7-383) 239 47 62. Fax (7-383) 234 21 63
E-mail: Yu.M.Shatunov@inp.nsk.su

Received 23 September 2003, revised 9 February 2004
Uspekhi Fizicheskikh Nauk **174** (4) 353 – 370 (2004)
Translated by G Pontecorvo; edited by A M Semikhatov

tion presented at conferences held in recent years [2 – 5]. The complete bibliography can be found in electronic libraries (see, e.g., Ref. [6]), therefore, only key references have been selected for presentation here.

2. Compton backscattering method and its realization at various electron storage rings

The method of Compton backscattering was proposed in 1963 in Refs [7, 8], in which the main beam characteristics obtained in collisions of laser photons with electrons were computed. This method was then confirmed experimentally at the Lebedev Institute (FIAN) [9] and studied in detail in Frascati (Italy). With the first installation Ladone [10] constructed there, a beam of Compton photons started to be used in nuclear physics. Widespread application of the method of Compton backscattering started in 1994 in Novosibirsk, where a series of studies on photon absorption and nuclear fission induced by photons was carried out at the ROKK installation (Inversely scattered Compton quanta) in collaboration with the INR RAS, Moscow [11]. At present, active work on photonuclear reactions in Compton beams is under way at Brookhaven (USA) with the LEGS device (Laser Electron Gamma Source) [12], in Grenoble at the ESRF storage ring (experiment GRAAL — GRenoble Accelerateur Anneau Laser) [13], in Japan at SPring-8 (installation LEPS — Laser Electron Photon Source [14]), etc. Important advantages of the beams used in these works (in addition to monochromaticity provided for by the tagging system) are coherence and high level of polarization, which allow investigating the spin structure of nucleons and various polarization effects in photon scattering on nuclei and nucleons. At present, attention is mainly drawn to measurements of the Gerasimov – Drell – Hearn (GDH) sum rule and of other sum rules that provide fundamental information on the anomalous magnetic moment and other properties of the nucleon.

It must be noted that polarization experiments are also actively implemented with photon beams obtained from the Bremsstrahlung of polarized electrons or from processes of Mueller scattering. Here, the work with Bremsstrahlung beams under way in Mainz and at TJLab (see, e.g., the reviews in Ref. [6]) is ahead of similar research with Compton installations. Besides the necessity of obtaining results via different methods, research with Compton photons can also be justified by the better quality of beams, i.e., a higher degree of gamma-quantum polarization and a lower background level, and, consequently, enhancement of the experimental precision.

The production of Compton beams requires electron storage rings in which the electron current amounts to several hundred milliamperes. The gamma-beam intensity is here relatively low (up to 10^7 photons s^{-1}). The bound is imposed on the intensity because electrons are knocked off the orbit of the storage ring and the beam lifetime is reduced. A large number of users work simultaneously at a given electron storage ring (the source of synchrotron radiation), and therefore the admissible reduction of the beam lifetime is usually agreed upon by all users and amounts to a value close to 15%.

It must be noted that in photonuclear studies in the intermediate energy range, additional restrictions on the beam intensity occur because of the limits to the rapidity of the electronics applied and to the capacities of the data acquisition and handling system; on the whole, all these conditions are quite consistent with each other.

The issue of enhancing the intensity of a gamma-beam has already been discussed (see, e.g., Ref. [15]). Clearly, the application of long-wave lasers, with relatively small electron energy losses due to the emission of gamma-quanta, can enhance the intensity if a scattered electron is not lost in the storage ring and returns to its equilibrium orbit. In this case, there in principle exist no limits to the beam intensity. The first successful experimental results in this sector were obtained in Japan at several electron storage rings making use of long-wave CO_2 lasers [16] and in the USA at Duke university with the aid of a laser on free electrons [17]. Because of the importance of this issue, especially for applied research, we discuss it in a separate section below.

Among the projects for future installations of a similar type, we note the 'Gamma' station that is under construction at the Kurchatov center of synchrotron radiation (KCSR) at the electron storage ring 'Sibir-2' [18]. This will be the first specialized SR source in Russia, and the creation of a beam of hard gamma-quanta here is an important task.

2.1 Principal characteristics of the Compton backscattering process

The differential cross section of Compton backscattering of laser photons on electrons of energy E_e in the laboratory reference system (given ideal conditions, with the emittance and transverse dimensions of the electron beam being infinitesimally small) can be represented, in accordance with calculations [7, 8], as

$$\frac{d\sigma}{dn} = 4\pi r_0^2 \left[\frac{K}{1+n} + \frac{1+n^2}{K} - \frac{4n^2}{(1+n^2)^2} \right], \qquad (1)$$

where $n = \theta\gamma$, $\gamma = E_e/m_e$, $\lambda = 2\gamma\omega/m_e$, $K = 1 + n^2 + \lambda$, ω is the energy of laser photons, and θ is the outgoing angle of a gamma-quantum with respect to the electron momentum.

The energy of a Compton gamma-quantum is uniquely related to its scattering angle:

$$E_\gamma = 4\gamma^2 \frac{\omega}{1+n^2+\lambda}. \qquad (2)$$

These formulas imply that the major part of the photon beam occupies a small angle $\theta \sim 1/\gamma$. In most of the existing installations, the electron energy amounts to several gigaelectronvolts, and therefore the characteristic angle does not exceed 10^{-3} rad.

The spectrum of gamma-quanta is described by the equation

$$\frac{d\sigma_0}{dE_\gamma} = \frac{\pi r_e^2}{2} \frac{m_e^2}{\omega E_2} \left[\frac{m_e^4}{(4\omega^2 - E_\gamma^2)^2} \frac{E_\gamma}{E_e - E_\gamma} - \frac{m_e^2}{\omega E_e} \frac{E_\gamma}{E_e - E_\gamma} + \frac{E_e - E_\gamma}{E_\gamma} + \frac{E_e}{E_e - E_\gamma} \right]. \qquad (3)$$

The polarization of the Compton gamma-quanta is determined by that of the laser photons. The cross section accounting for the photon polarization (for scattering on nonpolarized electrons) can be expressed through the Stokes parameters $\xi = (\xi_1, \xi_2, \xi_3)$, where $\xi_3 = 1$ corresponds to the horizontal linear polarization, $\xi_3 = -1$ corresponds to the vertical linear polarization, and ξ_1 and ξ_2 characterize the linear polarization at the angle 45° and the circular polariza-

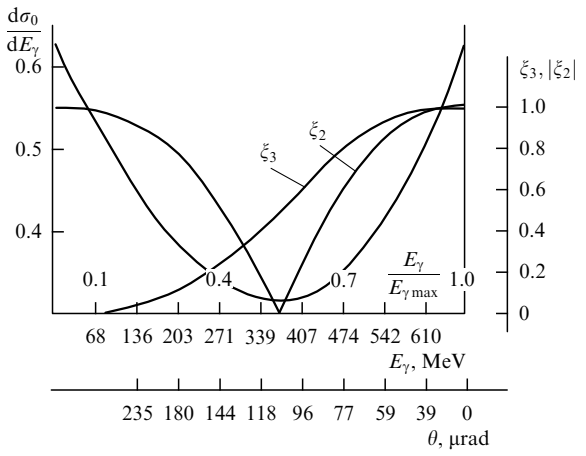

Figure 1. The spectrum $d\sigma_0/dE_\gamma$ (left scale) and polarization (ξ_3 — linear, ξ_2 — circular) (right scale) for Compton backscattered radiation [11].

tions, respectively:

$$d\sigma = d\sigma_0 - \frac{4r_e^2\, d\varphi\, dy}{x^2}\,\xi_3\left[\left(\frac{1}{x}-\frac{1}{y}\right)^2+\left(\frac{1}{x}-\frac{1}{y}\right)\right]. \qquad (4)$$

Here, φ is the azimuthal angle and the variables x and y are determined by the respective initial and final photon and electron momenta (k, k') and (p, p') as $x = 2pk/m^2$ and $y = 2pk'/m^2$.

The energy dependence of the linear and circular gamma-quantum polarizations is shown together with the spectrum in Fig. 1. It is seen that at the maximum energy, which corresponds to a scattering angle of 180°, the polarization equals 100%.

The most detailed calculations of the parameters of Compton photon beams can be found in Ref. [19]. The results of computations for measuring the gamma-beam polarization (of a polarimeter based on e^+e^--pair production in atomic electrons) are also given there. No experiments have been carried out yet for direct measurement of the polarization of gamma-quanta of intermediate energies. Therefore, the results of calculations in Ref. [19] may be applied in future work.

2.2 Parameters of experimental devices

The main parameters of the existing installations with Compton photon beams of intermediate energies are presented in Table 1. It is seen that these devices cover an energy range up to 3.5 GeV. The beam intensity does not exceed 10^7 photons s^{-1}, which is determined by admissible losses of the beam lifetime inside the storage ring, as noted above. To obtain a Compton beam with a high level of monochromaticity in energy, the method of tagging, i.e., of registering scattered electrons in coincidence with the nuclear reaction products, is additionally applied. A continuous or high-duty-cycle beam is preferable for this purpose.

The distance between electron bunches in modern storage rings, used as dedicated sources of synchrotron radiation, may be of the order of magnitude of one nanosecond for bunches several dozen picoseconds long, while the orbit may even be a kilometer or more long. Therefore, from the standpoint of the detecting system (with the time resolution in registration of electron coincidences with nuclear reaction products taken into account), such a beam can be considered continuous. But even in a single-bunch operation mode, the repetition rate is sufficient for the tagging system to function with a limited intensity.

Different installations involve differing tagging systems, which vary both in the sort of detectors used for registering scattered electrons and in the elements of the storage ring that require special upgrading. At Brookhaven, the LEGS setup makes use of a long channel for guiding the scattered electrons toward the plastic scintillators through a specially constructed lens [12]. At all other installations listed in Table 1, the detector of scattered electrons is mounted behind the magnet of the storage ring in the immediate vicinity of the electron beam axis. Figure 2 presents the example of the layout applied in Novosibirsk for the ROKK-2 setup.

It must be noted that gamma-installations (see Table 1) are available at all synchrotron radiation centers and at many electron–positron colliders. This is not only due to the interest in research on the interaction of gamma-quanta with nuclei, but also because Compton sources are useful for diagnosing the operation of the storage rings themselves. At present, Compton scattering is applied in measuring transverse and angular dimensions of beams, for determining the position and stability of the beam orbit, and for measuring the polarization of electrons inside the storage ring. These parameters are very important for tuning the storage ring and, consequently, for numerous experiments carried out on it.

It is interesting to compare the principal parameters of gamma-beams obtained by the method of Compton backscattering (see Table 1) and of Bremsstrahlung beams of tagged photons available at modern accelerators such as

Table 1. Parameters of installations with Compton backscattered photon beams.

Setup	Ladone	Taladone	ROKK			LEGS	GRAAL	LEPS
			1	2	1M			
Storage ring	Adone (Frascati)		VEPP-4, 3, 4M (Novosibirsk)			NSLS (Brookhaven)	ESRF (Grenoble)	SPring-8 (Osaka)
Electron energy E_e, GeV	1.5	1.5	1.8 – 5.5	0.35 – 2.0	1.4 – 5.3	2.5	6.04	8.0
Electron current I_e, A	0.1	0.1	0.2	0.1	0.2	0.2	0.1	0.2
Energy of laser photons W, eV	2.45	2.45	2.34 – 2.41	2.41 – 2.53	1.17 – 3.51	3.53	3.53	3.5
Energy of Compton quanta E_γ, MeV	5 – 80	35 – 80	100 – 960	140 – 220	100 – 1200	180 – 320	550 – 1470	150 – 2400
Energy resolution ΔE_γ (FWHM), MeV	0.07 – 8	4 – 2	1.5 – 2	4		6	16	30
Intensity, N_γ s^{-1}	10^5	5×10^5	2×10^5	2×10^6	2×10^6	4×10^5	2×10^6	10^7

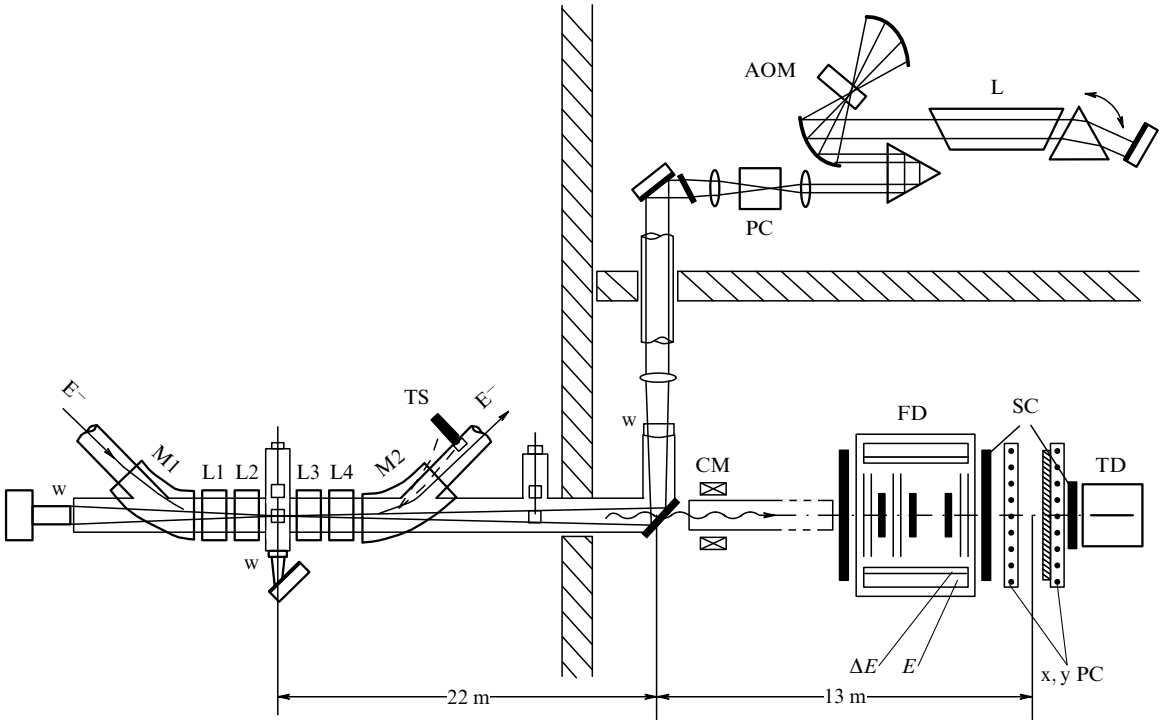

Figure 2. Layout of the ROKK-2 setup at the electron storage ring VEPP-3 [11], comprising three main parts: (1) the tagging system of photons by their energy (TS) mounted on the storage ring (M1, M2 are magnets, L1 – L4 are quadrupole lenses, w is a quartz window), (2) the laser system, including a laser L, and acoustic-optical modulator (AOM), a Pockels cell (PC), and optical elements (prism, lenses, mirrors), (3) the detecting system, where FD is the detector of nuclear fragments, CM is the cleaning magnet, SC, x, and y PC are beam monitors, and TD is a total-absorption photon detector.

CEBAF, producing 4 GeV electrons (LJLab laboratory in the USA) or MAMI-B with 850 MeV beams (FRG). The main technical difference consists in Bremsstrahlung beams being obtained here at an external target, to which the electron beam is guided from the accelerator. The electron beam in a storage ring crosses the radiation region a large number of times (with a frequency up to 50 MHz and even higher in the multibunch operation mode), and the electron beam intensity therefore reaches hundreds of milliamperes. In the tagging mode, the intensity of an extracted electron beam does not exceed several dozen nanoamperes. On the average, the intensities obtained from presently used Bremsstrahlung photon beams exceed the intensities of Compton beams by approximately one order of magnitude. But because the Compton spectrum rises with the photon energy, while the Bremsstrahlung spectrum drops off sharply, the flux of Compton photons in the hardest part of the spectrum near the upper boundary turns out to exceed the flux of Bremsstrahlung photons by an order of magnitude. Therefore, presenting only average values typically used for comparison is not quite correct.

Of special importance is the fact that the Compton spectrum exhibits no low-energy tail creating a harmful load for the tagging system and an additional background in the detector.

Concerning the remaining parameters, practically no essential differences exist between Compton and Bremsstrahlung beams. The energy resolution determined by the tagging system, on the average, amounts to about 1%. In both cases, a high polarization is achievable, close to 100% for a Compton beam and about 75% for a Bremsstrahlung beam (in the region of the maximum spectrum boundary). In this case, a Bremsstrahlung beam is obtained using a beam of accelerated polarized electrons, with the polarization reaching 75%.

Thus, the quality of beams of gamma-quanta and their possibilities mainly depend on background conditions; as the photon energy increases, the advantages of Compton beams, which are 'cleaner' and more effective, evidently become more noticeable. At the same time, extracted electron beams are, in the main, more oriented toward research on electromagnetic interactions of nuclei and nucleons by the method of electron scattering (virtual photons), which, in turn, yields unique information on the structure of nuclei. A more detailed comparison goes beyond the scope of the present review, and the reader is referred to the proceedings of conferences held in recent years [2 – 5].

3. Photonuclear research

The range of studies presently under way with Compton beams of intermediate energies is quite broad. We deal in greater detail with the work on photoabsorption by actinide nuclei carried out in Novosibirsk with the ROKK-1 and 2 installations [20 – 24], and also on elastic scattering of photons by nuclei [25, 26]. The results of the Novosibirsk experiments on photoabsorption by nuclei, confirmed by other investigations performed just recently, allow adopting a new standpoint concerning the absorption of photons by heavy nuclei or by bound nucleons. We here consider a revision of the concept of 'universality' in photoabsorption by nuclei in the region of nucleonic resonances. Then, we discuss certain results of the research on photoabsorption and photoproduction of mesons carried out at Brookhaven [27 – 29] and Grenoble [30 – 32] at the electron storage rings NSLS and ESRF, respectively.

Some results obtained at the storage ring SPring-8 [33–36] are also presented briefly.

In spite of the apparently different subjects of the listed experiments (nuclear photofission, meson photoproduction, elastic photon scattering), it must be noted that they all pertain to the common task of research on the interaction of photons with nuclei, namely to the study of total photoabsorption on free and bound nucleons. For example, data on fission provide information about the total cross sections of photoabsorption, since the fissilities of actinide nuclei are close to unity in the energy range considered. To analyze photoabsorption cross sections on heavy nuclei (or bound nucleons), data are required on photoabsorption by free nucleons, which in turn represent the sum of partial meson photoproduction cross sections. Finally, elastic and quasielastic scattering of photons on nucleons provides information about nuclear form factors, which determine the differences between free and bound nucleons. Therefore, a review of these issues is important for understanding the physics of nucleonic and mesonic degrees of freedom and for investigating the influence of a nuclear medium on the character of elementary processes.

3.1 Photofission of actinide nuclei

Until recently, numerous experimental data on the total cross sections of photoabsorption by nuclei from ^{7}Li up to ^{238}U, obtained at energies above the pion production threshold, pointed to the universal character of the dependence of the total cross sections on the atomic number of the target nucleus (see, e.g., review [37]). As shown in theoretical works (see, e.g., Refs [38, 39]), the influence of the nuclear medium (namely, the Fermi motion of nucleons, the Pauli principle, intranuclear cascades) is manifest in the deformation of differential cross section distributions, in the change of positions of nucleonic resonance maxima, and in other modifications, but in the integral cross sections, no noticeable differences exist between the total cross sections of photoabsorption on free and bound nucleons.

Of the actinide nuclei (thorium, uranium, neptunium, americium, and others), most attention in experiments was given to the ^{238}U nucleus (see, e.g., Ref. [1]). As noted in all publications, the total cross section of ^{238}U photofission within the energy range indicated coincides with the total photoabsorption cross section, in qualitative agreement with nuclear fissility known to rise with excitation energy. Experiments in beams of tagged photons have confirmed this conclusion with a precision close to a few per cent [40, 41].

No interest in heavier transuranium nuclei was observed, because for all actinide nuclei exhibiting low fission barriers, fissility measured as the ratio of the fission cross section to values on the universal curve was expected to be unity in the region of the nucleonic resonances. Therefore, the first announcement from Kharkov concerning the fissility of ^{241}Am and ^{243}Am nuclei in this energy range [42], which contradicted the conventional ideas concerning the universal character of photoabsorption, for a long time only gave rise to critical judgement. In Ref. [42], the photofission cross section for the ^{241}Am and ^{243}Am nuclei was claimed to be larger that the photofission cross section of ^{238}U by 30% in the region of intermediate energies, which served as an indication of possible additional mechanisms for the excitation of nuclei by photons of intermediate energies, other than the hadron channel related to meson photoproduction.

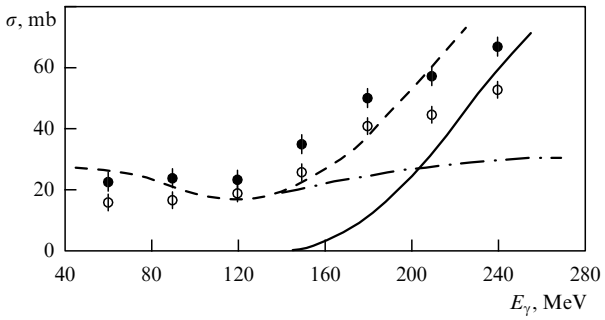

Figure 3. Photofission cross sections for ^{237}Np (●) and ^{238}U (○) nuclei based on data in Ref. [24]. The dashed curve represents the calculated cross section comprising two components — the total cross section of photoabsorption on a free proton [46] (solid curve) and the cross section of photoabsorption calculated by the quasideuteron model [51] (dot-dash curve).

The first studies carried out with the beam of Compton photons in Novosibirsk [20] confirmed the data in Ref. [42]. The use of a beam of monochromatic photons obtained by the Compton backscattering method reduced the probability of systematic errors in the measurement of relative fissilities of ^{238}U and ^{237}Np nuclei by several times, and therefore the deviation (30%) was 5 times larger than the total measurement error. The results of these measurements are presented in Fig. 3.

New experimental data have been obtained in Canada and the USA [43, 44] with beams of tagged Bremsstrahlung photons. These data confirmed the results concerning the different fissilities of ^{238}U and ^{237}Np nuclei in the region of intermediate energies. Moreover, the number of isotopes studied was increased (of the actinide nuclei, ^{233}U, ^{235}U, and ^{232}Th were added). Therefore, explanation of the observed divergence from the universal dependence of cross sections became even more important.

Theoretical estimates of fissilities based on the intranuclear cascade model (see, e.g., Ref. [24]), have shown that fissility of the uranium nucleus may be 30% lower than unity, owing to fission of the nucleus occurring at the last, slow stage of interaction, after the intranuclear cascade has terminated and static equilibrium has been established in the nucleus. The greater part of the energy is then carried away from the nucleus by fast pions and cascade particles. This model, clearly contradicting experiments, required a detailed analysis of the fissilities of actinide nuclei and of the total photoabsorption cross sections based on the cascade-evaporation model [45]. The result of such an analysis is presented in Fig. 4, where the solid curve describes the total photoabsorption cross section for nuclei ^{232}Th, ^{238}U, ^{235}U, and ^{237}Np, obtained from measured photofission cross sections, while the separate points correspond to the universal curve (the total photoabsorption for nuclei from ^{7}Li to ^{238}U based on the data in Refs [46, 48]).

Because all the total cross sections coincide with each other within the measurement errors (upon normalization to the number of nucleons in the nucleus, they land on the universal curve) for this range of nuclei, they are presented without additional discussion, as in Ref. [45].

It is essential that in measurements of the total photoabsorption cross sections for actinide nuclei, presented in Refs [43, 44], the accuracy of the data in terms of absolute cross sections is quite high (not worse than 3%). This level of

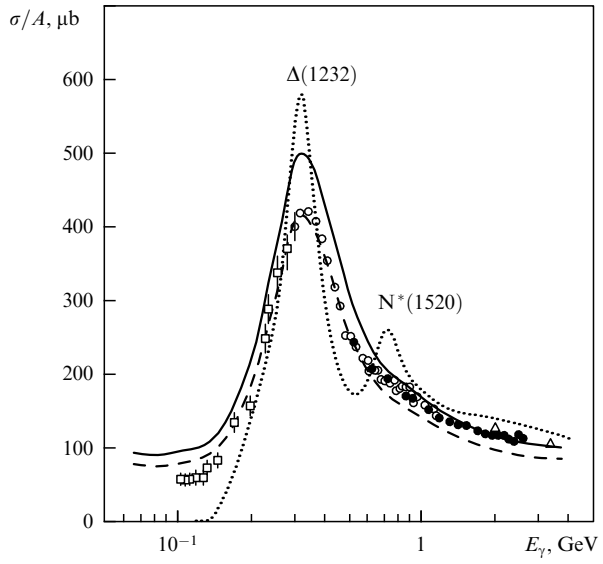

Figure 4. Total photoabsorption cross sections for actinide nuclei (averaged over ^{237}Np, ^{238}U, ^{235}U, and ^{233}U) based on the data in Ref. [45] (solid curve) and obtained from the photofission cross sections for these nuclei [44] by division by the computed fissility, compared with the total cross section of photoabsorption on a free nucleon (dotted curve). The dashed curve is the universal curve, on which the individual points for nuclei from ^{7}Li to ^{238}U are situated, based on the data in Refs [46, 48].

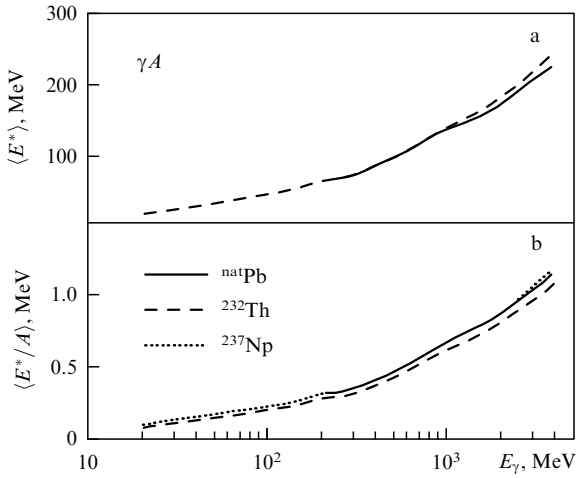

Figure 5. (a) Mean nuclear excitation energies after the intranuclear cascade ends versus the incident photon energy [45]. (b) The same after normalization to the number of nucleons in the nucleus. The notation is: ^{nat}Pb — solid curve, ^{232}Th — dashed curve, and ^{237}Np — dotted curve.

accuracy can be estimated by comparison of the total cross sections for a number of nuclei (^{232}Th, ^{238}U, ^{235}U, and ^{237}Np) for which the difference in the total photoabsorption cross sections has turned out not to exceed several per cent, although the photofission cross sections differ by more than a factor of two in this energy range (^{232}Th and ^{237}Np).

Several conclusions can be drawn from the presented data. First, modification of the nucleonic resonances in the nuclear medium is clearly seen: the $\Delta(1232)$-resonance becomes broader by nearly 50 MeV and the $N^*(1520)$-resonance disappears completely. This is confirmed by earlier results [49, 50]. Here, in the region of the Δ-resonance, the total photoabsorption cross section for actinide nuclei goes 20% higher than the universal curve. This fact is not readily explained by simple modification of the resonance in the nuclear medium, because the total cross section cannot change. Consequently, the assumption can be made that there exist additional mechanisms for the interaction of photons with nuclei, not related to meson photoproduction.

In the energy range above the Δ-resonance, and especially above $N^*(1520)$, the total photoabsorption cross sections presented in Ref. [44] coincide with the universal curve, but lie systematically below the absorption cross section on a free nucleon. That the total absorption cross sections on a bound nucleon becomes lower than on a free nucleon can be explained by the vector dominance model (see, e.g., Ref. [51]), according to which the nucleus becomes less transparent to photons of energies above approximately 1 GeV, owing to the effect of hadronization, or photoproduction of heavy vector mesons.

It must be noted that reliable data on the total photoabsorption cross sections for free protons and neutrons are available in the energy range up to 800 MeV, where the results in Refs [46–48] can be compared with each other. At higher energies, the only existing data were obtained by Armstrong et al. [46, 47]. Recently, communications have appeared of measurement results obtained by the GRAAL collaboration [52] (they are discussed below), which allow correcting the cross sections up to an energy of 1.5 GeV. From these data, one can clearly see a third resonance for the proton at the energy 1.0 GeV, while it is practically absent for the neutron. This, most likely, means that the procedure for extracting neutron data from measurements made with deuterons should be corrected. In the case at issue, comparison of the photoabsorption cross sections for nuclei and for a free nucleon must be performed precisely with the proton, not with the averaged sum for protons and neutrons, as in Ref. [45].

It is also necessary to bear in mind that estimation of the total photoabsorption cross sections for the actinide nuclei in Ref. [45] is based on model calculations of the fissilities of these nuclei (Fig. 5). Although the number of isotopes investigated is quite large (^{232}Th, ^{238}U, ^{235}U, and ^{237}Np) and the respective total cross sections thus obtained coincide, it would be desirable to carry out measurements of total cross sections in other, independent ways, for example, by summing the cross sections for partial reaction channels.

We recall that the main difference between the ^{238}U and ^{237}Np nuclei consists in the fission width of ^{238}U being 3 times less than that of ^{237}Np [53]. Fission widths characterize the probability of fission in the vicinity of the fission barrier, which amounts to approximately 6 MeV for both nuclei. The second, most probable, decay channel of a nucleus at this energy is the emission of a neutron. The total decay width is practically equal to the sum of the neutron (Γ_n) and fission (Γ_f) widths. Thus, in the vicinity of the fission barrier, the fission cross section can be described by the simple formula

$$\sigma_{\gamma f} = \sigma_{tot} \frac{\Gamma_f}{\Gamma_f + \Gamma_n} . \qquad (5)$$

As the photon energy increases, the probability of fission increases owing to fission of the nucleus also being possible after the emission of two, three, or more neutrons. The fissilities of the two nuclei reach saturation and approach unity at approximately 40 MeV, if all the photon energy is assumed to transfer into the excitation energy of the nucleus.

Detailed calculations performed with the emission of fast cascade particles taken into account [45] reveal that at higher energies, the fissility continues to grow, as shown in Fig. 5.

Additional information on the photoexcitation of nuclei, for instance, on the mean excitation energy of a fissioning nucleus, after the intranuclear cascade inside it ends, can be obtained by measuring the mass distributions of fission fragments. The asymmetry in the mass distribution of fragments is known to be related to shell effects, which play a noticeable role in the case of low excitation energies and become negligible at energies above about 50 MeV. Symmetric and asymmetric fission probabilities have been measured in Novosibirsk for the ^{238}U and ^{237}Np nuclei [21]. The results are presented in Table 2.

Table 2. Symmetric fission probability $R = S/(A + S)$ [22]; systematic errors are shown in parentheses.

E_γ, MeV	^{238}U	^{237}Np
60	0.25 (0.09)	0.22 (0.08)
90	0.32 (0.09)	0.21 (0.07)
120	0.29 (0.09)	0.30 (0.08)
150	0.39 (0.09)	0.25 (0.10)
180	0.35 (0.08)	0.35 (0.10)
210	0.37 (0.08)	0.38 (0.11)
240	0.34 (0.08)	0.12 (0.07)

The fraction of symmetric fission with respect to the total yield is seen not to exceed 40% for both nuclei, i.e., asymmetric nuclear fission predominates. Therefore, the qualitative conclusion can be made that the fraction of processes involving a low excitation energy of the fissioning nucleus is quite significant. This may imply that the results of calculations of the mean excitation energy of fissioning nuclei in Fig. 5 may be overestimated or that the dispersion of mean values is very large. The dispersion value is, regretfully, not presented in Ref. [45], and therefore no estimation of the fraction of low-energy excitations can be made.

A more detailed comparison also requires theoretical estimates of symmetric and asymmetric fission probabilities for the range of excitation energies of interest, which are still not to be found in the literature. Thus, available data on the mass distribution of photofission fragments only qualitatively confirm the possibility that a photoabsorption mechanism involving a small energy transfer exists and point to a difference between nuclear excitation processes induced by photons and by protons in the intermediate energy range.

Another qualitative indication that the issue of the mean excitation energy of fissioning nuclei has been studied insufficiently is given by the results of research on the excitation of spontaneously fissioning isomers by photons and electrons in the range of energies up to 1.2 GeV [54]. Isomeric states in fissioning nuclei are known to be due to shell effects responsible for the formation of double-humped fission barriers. When the excitation energy rises above approximately 30 MeV, the barriers become single-humped (liquid-drop) and the probability of isomers being produced drops down to zero.

The isomer ratio in the intermediate energy range is shown in Ref. [54] to be only several times lower than in the region of the giant resonance. This means that the mean excitation energy of fissioning nuclei does not exceed 30 MeV. Such a result is consistent with data on the mass distributions of fragments from photofissioning actinide nuclei.

On the basis of all the data presented, it is natural to assume that additional mechanisms of nuclear excitation exist that differ from the hadron mechanism, which is fully due to meson photoproduction on nucleons. However, searches for such mechanisms have not yet given positive results. An attempt was made in Ref. [18] to explain the excess of cross sections by rapid fragmentation of the nucleus, when nearly all the energy of the incident photon is transferred to the fragments without producing a compound nucleus. At low photon energies (up to 20 MeV), the probability of such a process does not exceed 10^{-5} with respect to the probability of the ordinary binary fission [55]. This quantity has also turned out to be very small (less than 10^{-3}) in the region of nucleonic resonances, according to the data in Ref. [18]. Consequently, processes involving large energy transfers cannot explain the excess in the total photoabsorption cross sections observed in the case of actinide nuclei.

Another explanation put forward is related to processes with small energy and momentum transfers [21], for example, inelastic electron – positron pair production, which is due to a long-range interaction (the Bethe – Heitler process). In recent years, the interest in such processes has grown in connection with investigation of the virtual Compton effect [56] and of the virtual pair photoproduction on nucleons [57].

The investigation of small-order (in the electromagnetic interaction coupling constant $\alpha = 1/137$) electrodynamic processes deserves to be discussed separately. Theoretical estimates of the probability of inelastic e^+e^--pair production, leading to actinide nuclei fissioning, yielded a cross section three orders of magnitude smaller than the experimental value [21]. It must be noted that the cross section of this process is strongly dependent on the nuclear form factor cutoff value, which has insufficient theoretical justification. Therefore, one of the arguments in favor of the necessity of studying the indicated process, independently of its relative probability, consists in the possibility of obtaining new information on the form factors of heavy nuclei. In this connection, it is interesting to analyze data on Coulomb dissociation of relativistic nuclei — a process that is essentially very close to the inelastic e^+e^--pair production on nuclei.

Diagrams corresponding to the inelastic e^+e^--pair production on a nucleus and to Coulomb dissociation of relativistic ions are presented in Fig. 6. It must be noted that

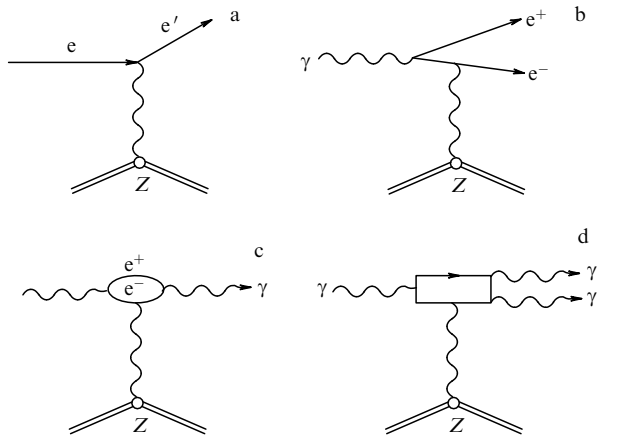

Figure 6. Diagrams for the following processes: (a) electron scattering or Coulomb dissociation of heavy ions, (b) inelastic e^+e^--pair production, (c) Delbruck scattering, and (d) photon splitting.

the diagram in Fig. 6b also describes electron scattering on nuclei, and therefore the theoretical description of both processes exhibits a common character. The processes indicated are conventionally analyzed by the method of virtual photons, a quite detailed description of which can be found, e.g., in Ref. [1]. In the Born approximation, the spectrum of virtual photons mainly depends on the initial and final momenta of the incident particle. Therefore, one can extrapolate the data on the cross sections to the small-Z region.

Extrapolation of the cross sections of Coulomb dissociation of relativistic heavy ions [59, 59] to the small-Z region reveals that the dependence of the cross section on the charge of the nucleus is quadratic, in agreement with theoretical estimations. The absolute value of the cross section of the inelastic e^+e^--pair production with the emission of a neutron or of fission (the probabilities of these processes in the vicinity of the barrier are close to each other) turns out to be approximately 10 mb.

The total photofission cross section for actinide nuclei then amounts to approximately 100 mb at the maximum of the P_{33}-resonance ($E_\gamma = 300$ MeV) and drops down to 50 mb at photon energies of about 1 GeV. Consequently, the data on cross sections obtained by the extrapolation method do not contradict the experimental results on the relative fissilities of uranium and neptunium nuclei presented above. Regretfully, the accuracy of such extrapolation is insufficient for definitive conclusions. Therefore, the full answer to the question concerning the reason for deviation of the total photoabsorption cross sections from the universal curve has yet to be found.

Thus, the most recent data on the photofission of actinide nuclei in the intermediate energy range have raised many questions that open important new sectors of research in this region. The main result can be considered to be that the 'universal' photoabsorption curve for heavy actinide nuclei is no longer universal. An explanation of this fact can be found in different ways, for example, by searching for processes such as inelastic e^+e^--pair production with small energy and momentum transfers or, contrariwise, in fragmentation processes of nuclei with large transfers.

This requires coincidence experiments involving the registration of fast nuclear products produced at the initial stage of interaction and of fission fragments providing information on the excitation of collective states. Such experiments can be performed with new-generation low-background photo-nuclear installations making use of gamma-quanta beams from laser photons Compton backscattered from electrons. Compton low-background beams in storage rings allow studying processes with small energy and momentum transfers. The existence of a nuclear vertex in these processes results in their very strong dependence on the nuclear form factor, which complicates theoretical analysis of the data. However, it is precisely this circumstance that allows obtaining additional information on the nuclear form factors. From this standpoint, processes with small transfers can be considered quasielastic.

A program of such experiments, based on the first data obtained at the Institute of Nuclear Physics of the RAS Siberian Branch (Novosibirsk), has been elaborated for the electron storage ring 'Sibir-2' at the Russian Research Center 'Kurchatov Institute' [60].

3.2 Elastic scattering of gamma-quanta on nuclei. Higher-order processes in the electromagnetic coupling constant $Z\alpha$

So far, the interaction of photons with nuclei has only been studied in lower orders in the coupling constant $Z\alpha$. Such processes include the well-studied Compton scattering and e^+e^--pair production. Processes of higher orders, like Delbruck scattering or photon splitting, whose diagrams are presented in Fig. 6, have been studied insufficiently.

Photon splitting on nuclei was first observed [25] in an experiment carried out at the VEPP-4 storage ring with the ROKK-1M setup. A special feature of this experiment consisted in the registration of photons in the region of small angles, i.e., on the background of the direct gamma-beam. Studies of Delbruck scattering were performed in a similar way [26]. The results of these experiments were shown to be in good agreement with electrodynamic calculations carried out in the approximation of plane waves and a point-like nuclear charge.

The differential cross section of Delbruck scattering on nonpolarized electrons can be represented as [26]

$$\frac{\mathrm{d}\sigma}{\mathrm{d}E_\gamma} = (Z\alpha)^4 r^4 \left[(A^{++})^2 + (A^{+-})^2\right], \qquad (6)$$

where r is the classical electron radius and A^{++} and A^{+-} are the conserved helicity and helicity-flip scattering amplitudes, respectively. At a high incident photon energy ($E_\gamma \gg m_e$) and small momentum transfer ($\Delta \ll E_\gamma$), corresponding to the conditions of the experiment performed, the quantity A is proportional to the energy E_γ, which allows a detailed comparison of theory and experiment. Theoretical estimation was performed applying various methods. In Refs [61, 62], Feynman diagrams were summed with the exchange of an arbitrary number of photons on the nuclear Coulomb charge taken into account. In Ref. [63], the classical approach was applied, giving results close to the ones obtained by the microscopic method. The results obtained in the experiments are in good agreement with theoretical calculations. Thus, elastic scattering of photons can be described with quite a good accuracy with higher orders [up to $(Z\alpha)^4$] of the relevant coupling taken into account. The nucleus is then taken to have a point-like charge and no internal structure.

Taking the nuclear form factor in photon elastic or quasielastic scattering processes into account represents a difficult task because nuclear interaction must be considered in addition to the electromagnetic operator. But this is precisely the path along which one may obtain new results concerning nuclear structure. As already mentioned above, the cross sections of processes like, for example, quasielastic e^+e^--pair production are more sensitive to the nuclear form factor than simple electromagnetic processes. This was first demonstrated in experiments carried out in Novosibirsk.

3.3 Cross sections and asymmetries of meson photoproduction on nucleons

The first systematic study of polarization effects in the interaction of photons with nucleons and nuclei in Compton backscattered photon beams was initiated at the LEGS (Laser Electron Gamma Source) installation in Brookhaven in 1990 at energies from 200 up to 320 MeV [27 – 29, 64 – 66].

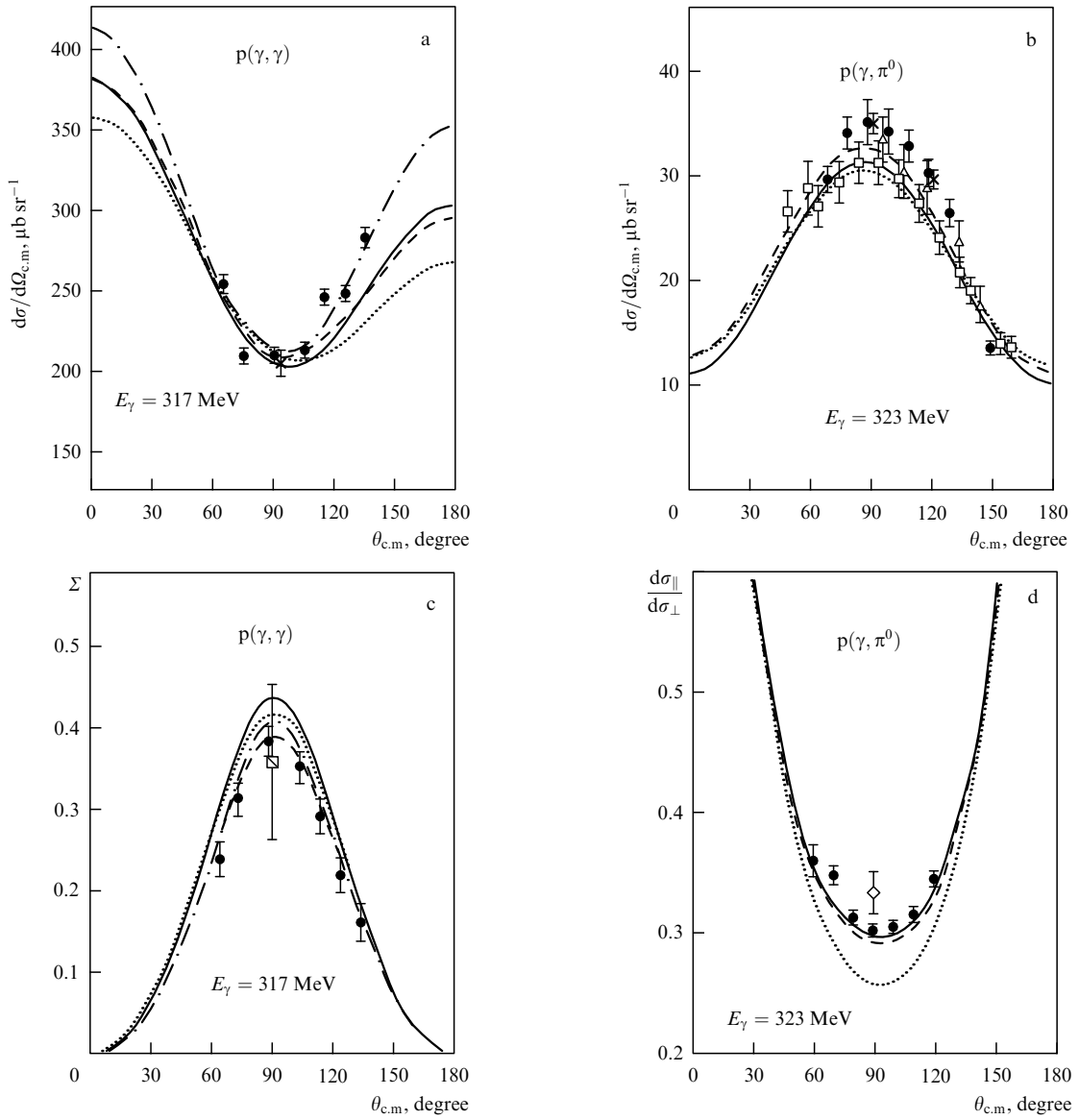

Figure 7. (a, b) Angular distributions for Compton scattering and π^0-meson photoproduction on the proton, respectively, from LEGS data (points [28]) and from Refs [68 – 73]. The curves represent various versions of theoretical calculations (for details, see Ref. [28]); (c, d) angular distributions and cross section ratios for Compton scattering and π^0-meson production on a proton, respectively, in a beam of polarized photons.

In the investigation of the structure of the nucleon, a new stage was launched, related to taking tensor interaction into account, which according to the quark model leads to mixing of quark spins with their relative motion. As a result, a D-wave component of the nucleon wave function arises, which violates spherical symmetry and leads to static deformation of the excited nucleonic states, for instance, of the Δ-resonance.

Because photons excite the Δ-resonance owing to the M1 interaction, while the quadrupole E2 component contributes relatively little, measuring the value and sign of the ratio of the components, E2/M1, turned out to be convenient for studying the internal structure of the nucleon. The main decay channel (99.4%) of excited nucleonic states in the energy region considered is pion production (πN), and only 0.6% correspond to transition to the initial state (Compton scattering). These branches exhibit different sensitivities to the contribution of the E2 component, which was studied experimentally at Brookhaven.

A liquid-hydrogen target was used in the experiments. Registration of recoil protons was performed using drift tracking chambers and a plastic time-of-flight spectrometer. Photons were detected by a high-resolution NAJ(Tl) detector. The results of measurements of angular distributions and of asymmetry (Σ) for Compton scattering and for neutral pion production are shown in Fig. 7. The polarization data define the value of G_E/G_M more precisely and allow determining the contribution of the E2 component to the N−Δ transition.

In recent years, the greatest interest has been aroused by studies of double polarization observables, when both polarized gamma-quanta and a polarized target are used. Recently, the first results have been obtained in Brookhaven on the asymmetries Σ, G, representing the beam asymmetry for a nonpolarized target at angles $0°/90°$ and $+45°/-45°$, and the E-helicity beam asymmetry.

In this case, the scattering cross section of polarized photons is expressed through the asymmetry coefficients Σ, G, and E and through the target polarization coefficient P_Z

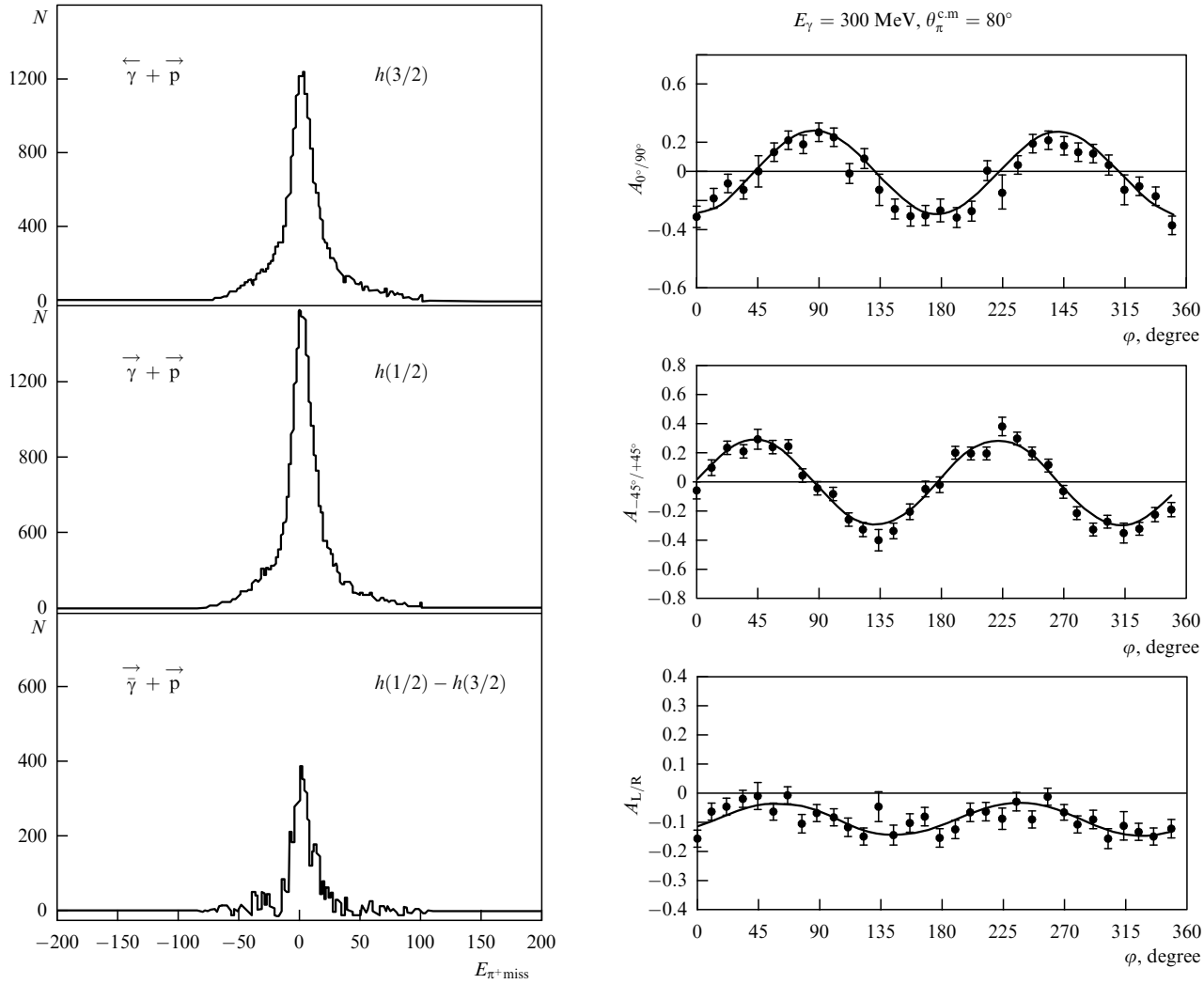

Figure 8. Left: missing mass spectrum for π^+-mesons from the polarized target in a beam of circularly polarized photons. $h(1/2)$ and $h(3/2)$ indicate parallel and antiparallel spins of the photon and proton, respectively. Right: asymmetry of π^+-meson photoproduction for the ratio $0°/90°$ (top) and $-45°/45°$ (middle) in a beam of linearly polarized photons; bottom right: asymmetry on circularly polarized photons. The curves are the result of approximation [67].

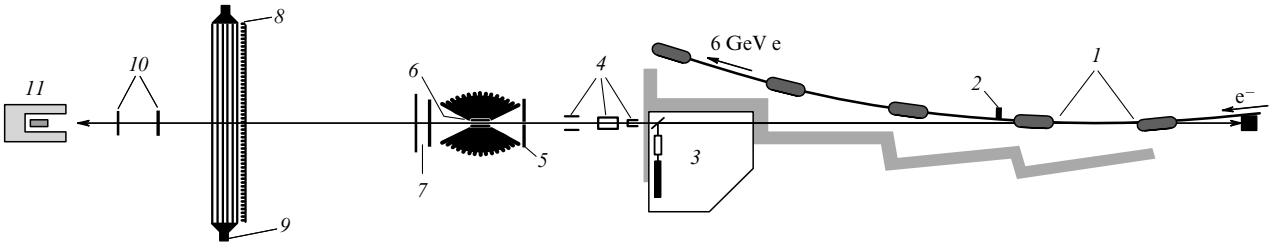

Figure 9. Principal elements of GRAAL setup [30]: *1* — interaction region of laser photons with electrons in the storage ring, *2* — tagging system, *3* — laser hatch, *4* — gamma-beam formation and cleaning system, *5* — wide-aperture detector of neutral and charged particles, *6* — target, *7* — proportional chambers, *8* — double wall of plastic scintillators, *9* — electromagnetic calorimeter, *10* — beam monitors, and *11* — total absorption spectrometer.

as [66]

$$\frac{\mathrm{d}\sigma}{\mathrm{d}\omega}(\theta,\varphi,E_\gamma) = \frac{\mathrm{d}\sigma}{\mathrm{d}\omega}(\theta,E_\gamma)\{1 + [Q_\gamma(E_\gamma)\,\Sigma(\theta,E_\gamma) - P_Z U_\gamma(E_\gamma)]\cos 2\varphi + [Q_\gamma(E_\gamma)\,G(\theta,E_\gamma)P_Z + U_\gamma(E_\gamma)\,\Sigma(\theta,E_\gamma)]\sin 2\varphi - P_Z V_\gamma(E_\gamma)\,E(\theta,E_\gamma)\}\,. \quad (7)$$

The coefficients $Q_\gamma(E_\gamma)$, $V_\gamma(E_\gamma)$, and $U_\gamma(E_\gamma)$ determine the Stokes vector $S_\gamma(Q_\gamma, V_\gamma, U_\gamma)$ of the gamma-beam. We here retain the notation adopted in Ref. [66].

Measurements were carried out with the polarized hydrogen – deuterium target SPHICE (Strongly Polarized Hydrogen deuteride ICE). It represents an HD molecular mixture in the solid phase, which allows achieving a polarization of about 80% for protons and 50% for deuterons at low temperatures (1.5 – 2 mK) in a strong

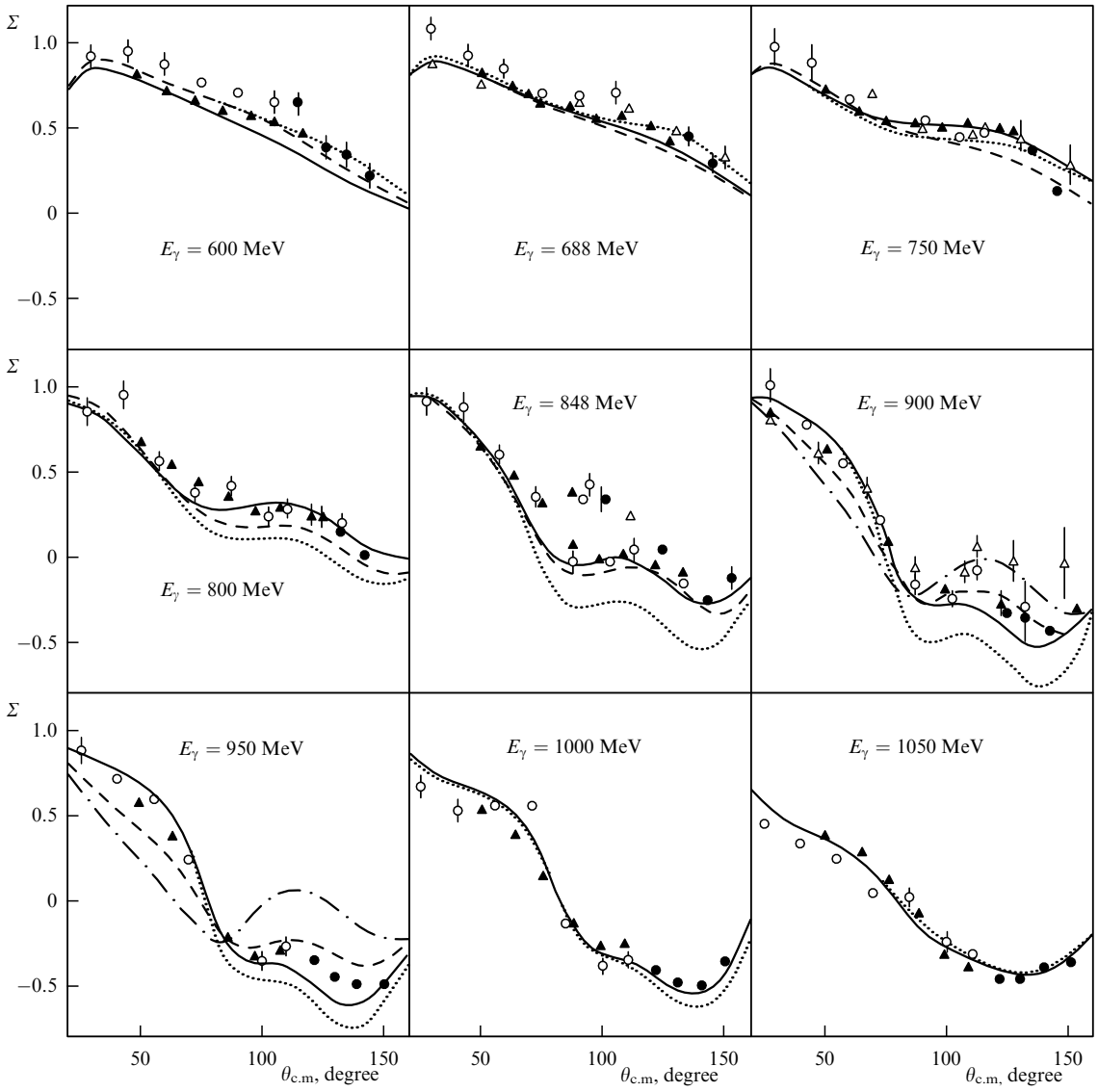

Figure 10. Asymmetry (Σ) for the π^+-meson production in the reaction $\gamma p \to \pi^+ n$ versus the outgoing pion angle in the center-of-mass system for incident photons of different energies. The dark circles and triangles indicate GRAAL results [31] as compared with the data of other authors [76–78]. The solid curves are the result of multipole analysis [79]. Dotted and dashed lines correspond to predictions of the isobar model [80].

magnetic field (15–17 T) [29]. For a circularly polarized gamma-beam, dependences of the positive pion yield for parallel and antiparallel nucleon and photon spins were measured.

The azimuthal dependence of the measured asymmetry coefficients Σ, G, and E is presented in Fig. 8. The low background is to be noted in these experiments. The obtained data are applied in testing the fundamental Gerasimov–Drell–Hearn sum rules and polarizabilities of the nucleon. The data on the sum rules were used for determining the anomalous magnetic moment of the nucleon (see, e.g., Ref. [6]).

The systematic research on meson photoproduction and the spectroscopy of excited nucleonic states was extended to the energy range of gamma-quanta up to 1500 MeV in the GRAAL experiment (Fig. 9) at the electron storage ring ESRF (Grenoble, France), where the investigation of strange particle and vector meson production became possible, which is interesting from the standpoint of nucleonic and mesonic degrees of freedom.

The beam parameters at the GRAAL setup, achieved by application of the Compton method, have been described above. The creation of a wide-aperture ($\approx 4\pi$) detector represents an important supplement to the gamma-beam. The main part of the detector is a sphere comprising 480 BGO crystals 21 radiation lengths thick, which provides an energy resolution of $0.0244E^{-0.47}$ (GeV) [74]. In order to separate neutral and charged particles, a plastic ΔE-detector consisting of 32 strips of plastic 5 mm thick and two cylindrical proportional chambers, which allow finding the interaction vertex of gamma-quanta with the target, have been placed between the BGO and the target. Particle registration in the forward direction (at scattering angles less than 25°) is performed with the aid of plane proportional chambers, two walls of plastic scintillators of area 9 m^2, and an electromagnetic calorimeter of plastic and lead layers [75]. The backward angles (exceeding 155°) are covered by a disk of two plastic and lead segments. Thus, particle registration with full solid angle coverage is ensured.

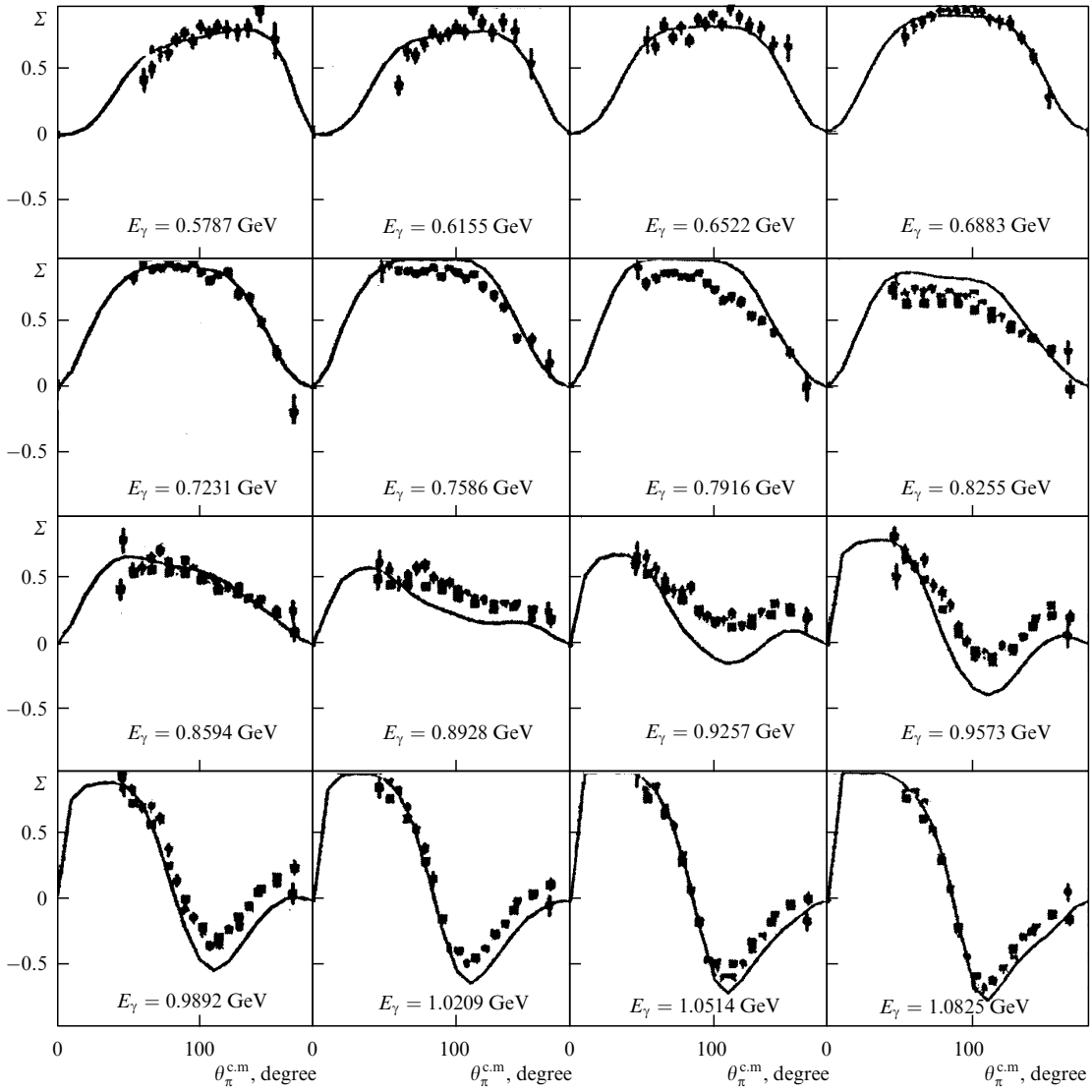

Figure 11. Asymmetry (Σ) for the π^0-meson production in the reaction $\gamma p \to \pi^0 p$ versus the outgoing pion angle in the center-of-mass system for incident photons of different energies from GRAAL results [81]. The solid curves are the result of multipole analysis [79].

The first publications by the GRAAL collaboration are devoted to investigation of the asymmetry of pseudoscalar meson photoproduction (of neutral and charged pions, as well as η-mesons) [44–46]. Measurements were performed with a beam of linearly polarized photons of energy from 500 to 1100 MeV with the use of an argon laser ($\lambda = 514$ nm) and 800–1500 MeV ($\lambda = 340$ nm). The energy ranges overlapping in the 800–1100 MeV energy region permitted controlling systematic errors and obtaining high-precision results. Figures 10 and 11 demonstrate the example of data on the asymmetry of meson photoproduction versus the angle $\theta^{\text{c.m}}$ for photons of various energies E_γ. Here, data are presented from different experiments in comparison with theoretical calculations.

The differential η-meson photoproduction cross sections [32] are shown in Fig. 12. The asymmetry can be seen to rise at an energy above 1 GeV, which is not predicted by the multipole analysis. This may point to the F_{15}-resonance contributing to the η-meson photoproduction in this energy range. On the whole, these results are important for describing the nucleonic resonances S_{11} (1525), D_{13} (1520), D_{15} (1700), and F_{15} (1580). Here, we have only presented a restricted number of results, permitting us to see the possibilities of photonuclear experiments for research in this field.

With the GRAAL setup, data have been obtained on the total photoabsorption cross sections on the proton and the deuteron in the energy range from 500 to 1500 MeV. Owing to the low background, two methods were applied: subtraction of the contribution of the empty target from the total hadron yield and summation of the partial cross sections determined by a kinematical analysis of the yields of reaction products. The results of measurements for the proton are shown in Figs 13 and 14. The data of Refs [46, 48], obtained earlier, are shown for comparison.

At energies below 800 MeV, the results of different experiments are seen to be in good agreement with each other. At higher energies, where data are scarce, new results allow describing the shape and absolute value of cross sections more accurately. This is important for analyzing total photoabsorption cross sections on heavy nuclei and for studying the vector dominance of photons. The systematic errors of measurements performed by the two methods do not exceed 5% at photon energies below 1 GeV. At higher

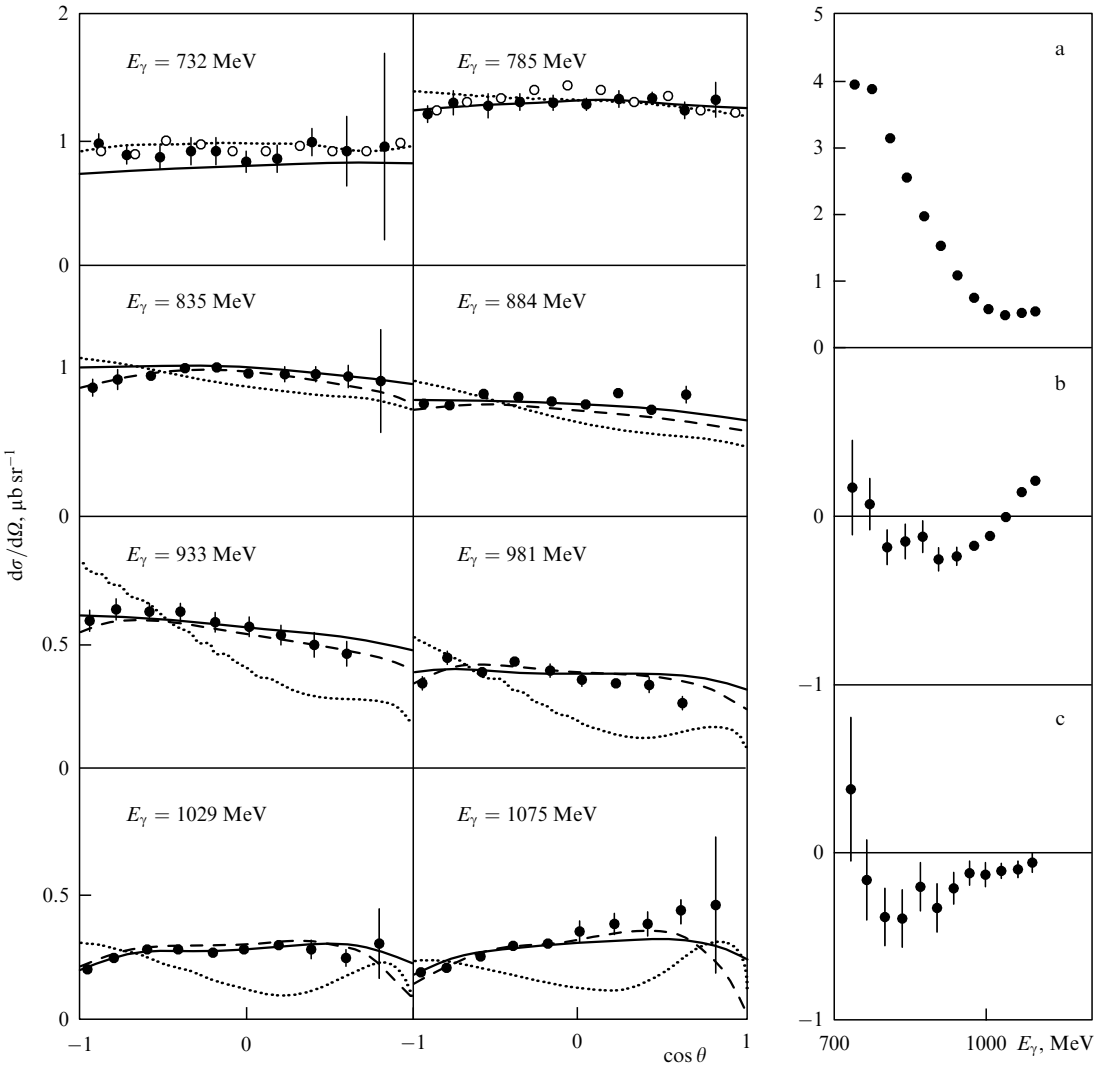

Figure 12. Differential photoproduction cross sections of η-mesons in the reaction $\gamma p \to \eta p$ versus the cosine of the outgoing pion angle in the center-of-mass system for incident photons of different energies. The solid and empty circles indicate GRAAL [32] and MAMI [82] results, respectively. On the right, a–c show results of approximation of the cross section by the formula $d\sigma/d\Omega = q/k(a + b\cos\theta + c\cos^2\theta)$. The dashed lines are the result of multipole analysis [79], the dotted and solid lines are predictions of theoretical models [82] and [83], respectively.

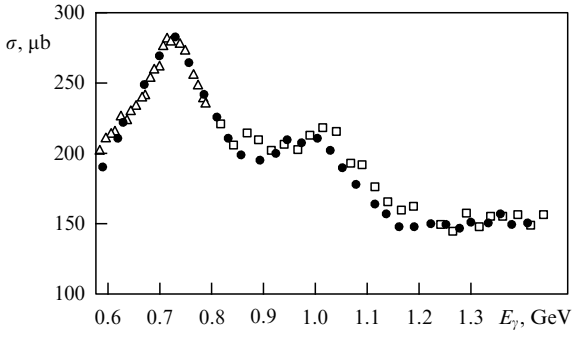

Figure 13. Total photoabsorption cross section on a proton: ● — data from Ref. [52], △ — [46], □ — [48].

energies, the contribution of partial channels with pion multiplicities $M > 2$ is not taken into account in the summation method.

It must be noted that the systematic error in the subtraction method is minimal throughout the whole energy range. Analysis of data by this method is described in detail in Ref. [52].

Figure 15 shows the total photoabsorption cross section of a deuteron (normalized to the number of nucleons equal to two) [52]. It is seen that the simple normalization does not allow obtaining the correct photoabsorption cross section on a neutron, and the influence of the second nucleon, i.e., the proton, must be taken into account. For this, one can, evidently, measure the total cross section on a quasifree proton applying the aforementioned method of summing partial reactions and then introduce the appropriate corrections. It is then natural to use the assumption that the influence of the neutron, as a spectator, on the proton and, vice versa, of the proton, as a spectator, on the neutron should be the same.

Further extension of research into the region of higher energies (up to 3.5 GeV) with the use of a beam of Compton backscattered photons has recently started at the SPring-8 accelerator with the LEPS setup (see, e.g., Ref. [50]). A special feature of this setup (Fig. 16) is the presence of a wide-aperture magnetic spectrometer permitting the effective separation of the charged photonuclear reaction products, as shown in Fig. 17. The main work with this setup during the past two years has been related to the investigation of the

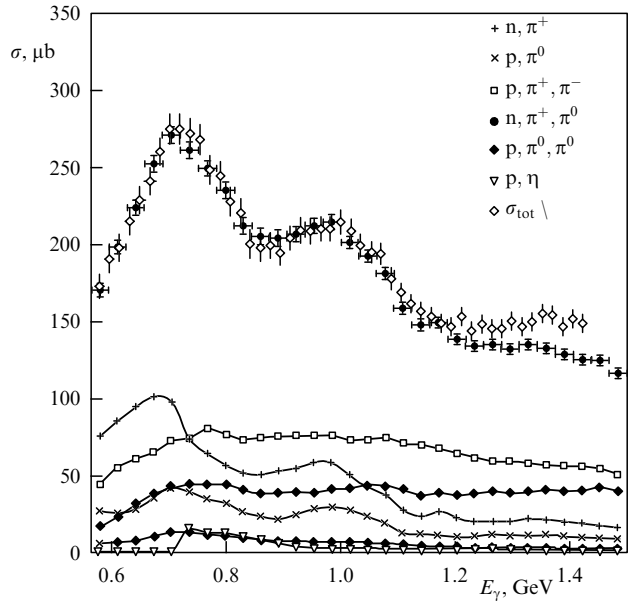

Figure 14. Total photoabsorption cross section on the proton, obtained by summing the partial pion photoproduction cross sections [84], compared with the cross section obtained by the subtraction method ($\sigma_{\rm tot}$).

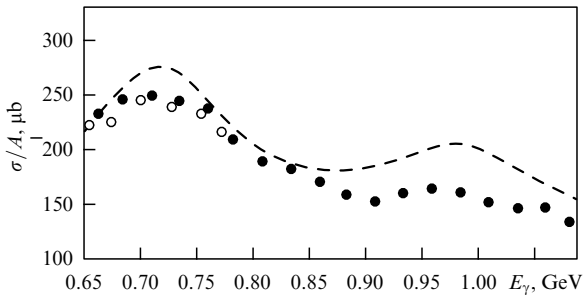

Figure 15. Total photoabsorption cross section on the deuteron (● — GRAAL data [52], ○ — [48]), divided by two, compared with the total photoabsorption cross section on the proton (averaged over the data presented in Fig. 13) — dashed line.

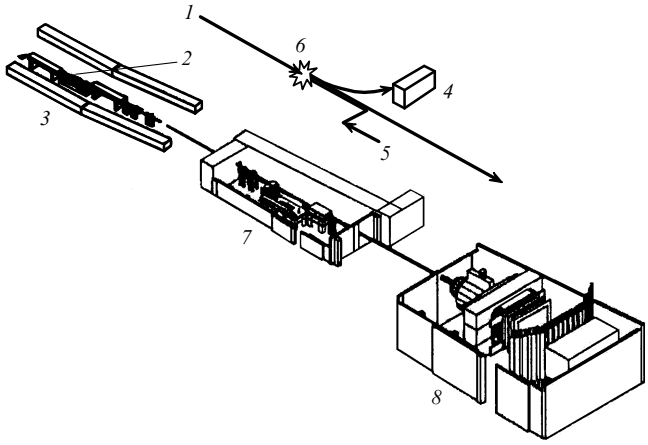

Figure 16. Layout of the LEPS setup [33]: *1* — beam of 1 GeV electrons, *2*, *6* — straight-line section of the storage ring (interaction region of the laser photons and electrons), *3*, *5* — laser system, *4* — tagging system, *7* — beam formation and cleaning system, and *8* — detecting system.

coherent φ- and ω-meson production processes on the proton and the deuteron [33], investigation of the asymmetry of kaon photoproduction in reactions $p(\gamma, K^+)\Lambda$ and $p(\gamma, K^+)\Sigma^0$ at $E_\gamma = 1.5-2.4$ GeV [50], and studying spin effects and the dynamics of φ-meson photoproduction [33–35].

Regretfully, the scope of this review does not permit us to consider this activity in detail. We only mention the most recent work where indications were obtained that a baryon resonance of strangeness $S = +1$ was observed in interactions of gamma-quanta with neutrons [85].

Among the promising ways of utilizing Compton beams of intermediate energies, the possibility must be noted of studying the interactions of short-lived mesons with the nuclear medium, namely, the method of tagged mesons [86]. This method is illustrated by Fig. 18. Owing to the energy and momentum conservation laws, recoil nucleons moving in the forward direction carry information on the mass of the meson produced. Results of simulation show that because the

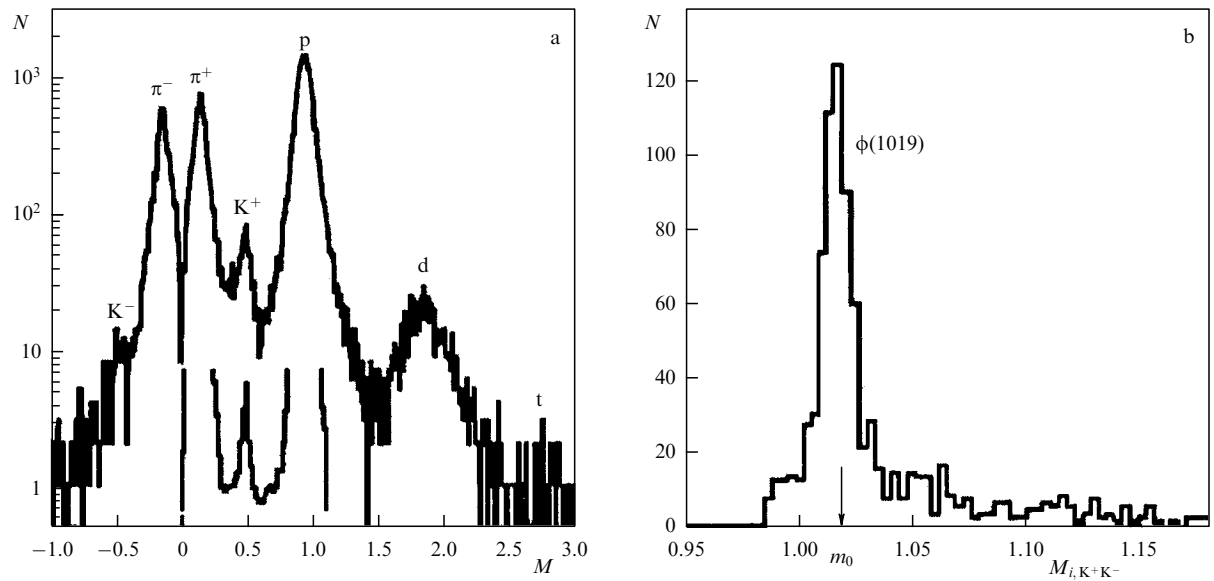

Figure 17. (a) Results of particle identification with the LEPS setup [35]. (b) Missing mass distribution for K^+-, K^--meson photoproduction.

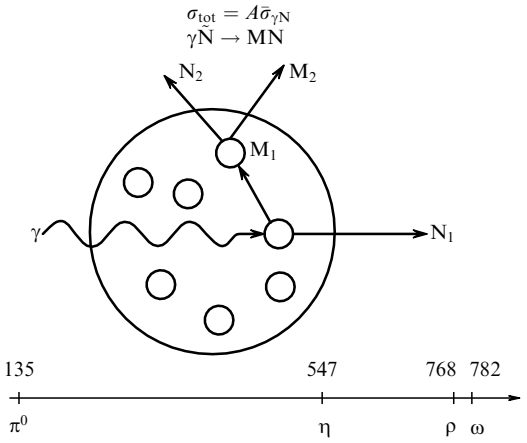

Figure 18. Method of meson tagging. The gamma-quantum interacts with a quasifree nucleon, which is detected in the forward direction with a high probability when a secondary interaction is absent. The meson produced interacts with nucleons of the nucleus and gives rise to secondary products.

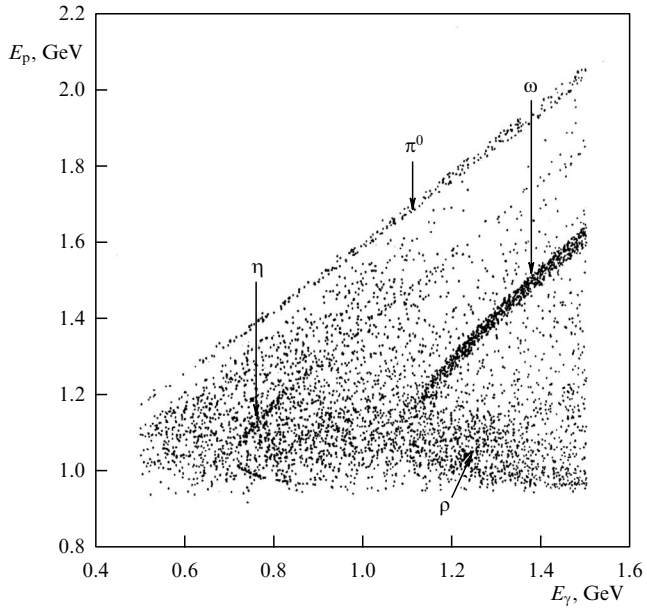

Figure 19. Results of simulation of secondary particle spectra from meson production [86]. The forward recoil proton energy versus the photon energy for various cases of meson photoproduction is shown.

Table 3. Probability of secondary particle emission from the ^{14}N nucleus, induced by the π^0- and η-meson photoproduction.

Particle	Stage of reaction	$\gamma p(^{14}N) \to \pi^0 p$	$\gamma p(^{14}N) \to \eta p$
P	1	95	95
π^0	1	80	0
η	1	0	70
P	2	22.0	20.8
N	2	23.7	22.1
π^0	2	8.7	8.6
π^+	2	8.7	9.1
π^-	2	7.8	6.8
P	3	8.9	7.2
N	3	8.9	7.1
P	4	2.6	2.2
N	4	2.9	2.0

difference in mass between mesons (π^0, η) is quite large compared with the experimental resolution (Fermi broadening of the spectrum and other factors hindering implementation of the experiment), the sort of meson can be identified by registering the recoil nucleons (Fig. 19, Table 3).

An essential condition for making such an experiment possible is a low background level, which can be achieved at installations with beams of Compton photons. A detailed analysis of the background conditions at the GRAAL setup was given in Ref. [52].

Figure 19 shows the results of simulation obtained for a free proton. The π- and η-mesons are seen to readily separate, because their masses differ quite significantly. This is also possible for other mesons, but a higher resolution is required. Taking the nuclear medium into account reveals that in the region of light and moderately heavy nuclei, the method can be applied, because the mechanism of quasifree meson production is predominant.

4. Production of intense gamma-quantum beams with the aid of long-wave lasers and lasers on free electrons

It was already mentioned above that an important achievement of recent years has been the creation of high-intensity beams obtained by the Compton backscattering method. The possibilities of this method are evident, and they were discussed earlier in Novosibirsk with an account of simulation results [15]. Practical success in this direction was first achieved in Japan making use of long-wave lasers [16], and then in USA with the aid of lasers on free electrons (the HIγS setup [17]).

The energy of a gamma-beam obtained with the aid of long-wave lasers is lower than in the case of short-wave lasers, but, in compensation, restrictions are no longer imposed on the beam intensity. There naturally remain technical problems related to the laser being very powerful.

Enhancement of the laser power from several Watts up to several kWatts in experiments [16] led to an increase in intensity by about 3 orders of magnitude (up to 10^9 photons s^{-1}). However, replacement of an argon laser with a CO_2 laser resulted in the maximum gamma-beam energy being reduced by a factor of 20, in proportion to the wavelength ratio.

Further enhancement of the intensity by 2–3 orders of magnitude (up to 10^{12} photons s^{-1}) was proposed and implemented by application of a laser on free electrons [17]. The beam monochromaticity was then ensured by collimation, because the energy and scattering angle of Compton photons are strictly related. The layout of the HIγS setup and the beam intensity obtained with it are presented in Fig. 20.

The mirrors of the resonator are placed such that the laser radiation bunch produced interacts with the successive electron bunch of the storage ring. Compton backscattering then occurs, and the gamma-quantum produced escapes in the direction of the electron momentum. The conditions for beam formation are optimal, because everything proceeds inside a single section of the storage ring, where the undulator is situated, and a high radiation power can be achieved.

The use of a laser on free electrons is seen to permit increasing the gamma-beam intensity by practically several orders of magnitude, up to 10^{12} photons s^{-1}, which opens new possibilities for utilization of Compton beams in various applied activities. This is especially important for radiation studies of materials and for studying the influence of

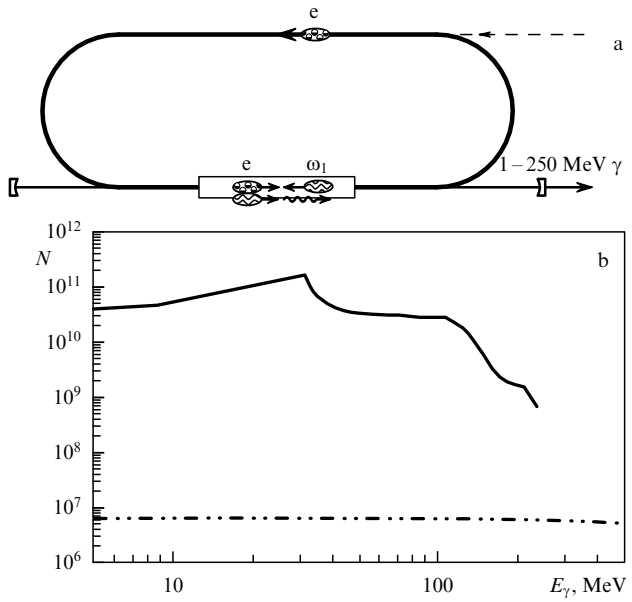

Figure 20. (a) Layout of the HIγS setup, with which a beam of Compton backscattered photons was obtained using a laser on free electrons [17]. (b) Compton backscattered photon beam intensity versus energy for the HIγS setup (solid curve) compared with the beam intensity obtained using an ordinary laser (dot-dash curve).

electromagnetic radiation on materials and biological objects. Clearly, the new technique, which provides for (besides high intensity) a high degree of monochromaticity, a small angular divergence, and tuning the beam energy within quite a broad range, offers much broader possibilities than the traditional gamma-sources based on Bremsstrahlung or characteristic emission.

As regards the fundamental research, the creation of an intense photon beam has permitted initiating astrophysical studies related to the measurement of deeply subthreshold reaction cross sections. For example, the investigation of photoneutron reactions on light nuclei (D, Be) at photon energies from 1 to 3 MeV yields information on the inverse reactions that are essential at the early stage of the universe formation [87]; by measuring the $^{16}O(\gamma,\alpha)^{12}C$ reaction cross section at energies from 1 to 3 MeV, it is possible to study the formation of oxygen and the burning of helium in stars.

5. The diagnostics of beams in storage beams with the aid of gamma-quanta

In conclusion, work should be mentioned in which Compton gamma-quanta are used for diagnosing the beams themselves in storage rings, especially that the first such setups were historically intended for measuring the degree of radiative polarization of electrons and positrons. This method of polarimetry, proposed in 1966 [88] and first realized at SPEAR [89] and VEPP-4 [90], is at present widespread and most often applied for determining both the transverse and the longitudinal polarization components at beam energies within the range from one to several dozen gigaelectronvolts (see, e.g., Refs [91 – 93]).

The small angular divergence of Compton backscattering and the features of its spectrum permit controlling the transverse and angular dimensions of the beam by measuring the space distribution of the most energetic gamma-quanta, which is unambiguously related to the distribution of particles in the interaction region.

Another method for measuring the dimensions of a beam at a micron and submicron level both in storage rings and in linear accelerators is possible by registering Compton gamma-quanta due to scanning with a narrow laser photon beam directed transversely to the motion of electrons. The limit resolution of this method ($\sim \lambda/\pi$) can be achieved by using interference of the laser beam [94].

When work is carried out with Compton gamma-quanta, Bremsstrahlung on atoms of the residual gas represents a background process. Knowledge of this background is not only necessary for experiments, but also expedient for tuning the storage ring itself. The circulating beam ionizes the residual gases present in the vacuum chamber, and the positive ions are captured by the attractive potential of the electron beam. Accumulation of ions in the case of a sufficient beam intensity results not only in deterioration of the effective vacuum, but also in possible mutual excitation of electron and ion oscillations, which leads to enhancement of the beam emittance and even to its partial destruction. Observation of the Bremsstrahlung, whose intensity is directly proportional to the ion density on the orbit, allows controlling these processes [95].

The examples presented far from exhaust all the useful applications of gamma-quanta at storage rings; however, a detailed discussion of work on this subject goes beyond the scope of this review.

6. Conclusion

In recent years, certain progress can clearly be seen in the development of new methods for obtaining gamma-beams of energies from several megaelectronvolts to several gigaelectronvolts, which is related to elaboration of the method of Compton backscattering of laser photons at electron storage rings.

The use of gamma-quanta of intermediate energies, with the wavelength comparable to the size of a nucleon, has allowed obtaining new important results on nuclear structure at the level of nucleonic and mesonic degrees of freedom. The differences from the universal curve revealed in the photoabsorption cross sections for actinide nuclei have raised many important new issues relevant to the physics of the nucleon and to the influence of a nuclear medium on the character of elementary processes. Owing to the low background, it has become possible to set the tasks to search for new baryonic states and to investigate the interaction of mesons with nuclei and nucleons.

Of special interest is the possibility of implementing coincidence experiments on actinide nuclei involving the registration of fast nuclear fragments and nucleons together with slow fission fragments, which will yield information on energy relaxation mechanisms in nuclei and transitions from the fast cascade stage of a reaction to collective dynamic equilibrium.

The creation of intense low-energy beams of gamma-quanta, based on the utilization of long-wave lasers, and especially of lasers on free electrons, essentially leads to expansion of the program of experiments, to the resolution of astrophysical problems, to the investigation of photoneutron reactions, etc. At the same time, such beams allow us to approach the resolution of important applied problems,

including the transmutation of elements and other problems of radiation research of materials.

Finally, installations with beams of hard photons at electron storage rings have demonstrated the possibility of their application for diagnosing the operation of the storage rings themselves, which is very important for optimization of the operation mode, accounting for the large user community.

Thus, the creation of high-quality gamma-beams on the basis of electron storage rings will doubtless be of great importance for the development of new ideas and promising technologies in years to come. A great part in developing these ideas and methods is due to the pioneer studies carried out in Novosibirsk.

To conclude, we would like to express hope that this review will serve as grounds for promising experiments to be implemented at electron storage rings. Certain possibilities are opening up in this direction, for instance, at the Russian Research Center 'Kurchatov Institute' owing to the creation of the first dedicated SR source in Russia.

The authors express their gratitude to V Litvinenko and M Fujiwara for putting material at their disposal, and to S T Belyaev, A N Skrinskiĭ, and A V Stepanov for interest in the work and useful observations.

The work was carried out with the support of the RFBR, grant 01-02-17235.

Author's note to English proofs

The authors would like to pay tribute to the memory of Professor G Ya Kezerashvili, whose pioneering work at Novosibirsk greatly contributed to the backscattering technique and intermediate-energy nuclear physics.

References

1. Nedorezov V G, Ranyuk Yu N *Fotodelenie Yader za Gigantskim Rezonansom* (Photofission of Nuclei beyond the Giant Resonance) (Kiev: Naukova Dumka, 1989)
2. Fujiwara M, Shima T (Eds) *Proc. of the Intern. Symp.* "*Electromagnetic Interactions in Nuclear and Hadron Physics*", *Osaka, Japan, 4–7 Dec. 2001* (River Edge, NJ: World Scientific, 2002)
3. Drechsel D, Tiator L (Eds) *NSTAR 2001*: *Proc. of the Workshop on the Physics of Excited Nucleons, Mainz, Germany, 7–10 March 2001* (Singapore: World Scientific, 2001)
4. *Backscattered Photon Workshop* (Frascati, 2002) (unpublished)
5. Gurevich G M (Ed.) *Proc. of the X Intern. Seminar on Electromagnetic Interactions of Nuclei at Low and Medium Energies* (*EMIN-2003*), *Moscow, April 16–18, 2003* (in press)
6. SPIRES HEP Literature Database, http://www.slac.stanford.edu/spires/hep/
7. Arutyunyan F R, Tumanyan V A *Zh. Eksp. Teor. Fiz.* **44** 2100 (1963) [*Sov. Phys. JETP* **17** 1412 (1963)]
8. Milburn R H *Phys. Rev. Lett.* **10** 75 (1963)
9. Kolesnikov L A, in *Elektromagnitnye Vzaimodeĭstviya Yader pri Malykh i Srednikh Energiyakh*: *Trudy 4-go Seminara, Moskva, 1977* (Electromagnetic Interactions of Nuclei at Low and Intermediate Energies: Proc. of the 4th Seminar, Moscow, 1977) (Editor-in-Chief G M Gurevich) (Moscow: Nauka, 1979) p. 338
10. Pascale M P et al., in *Proc. of the 4th Course of the Intern. School on Intermediate Energy Nuclear Physics, San Miniato, Italy, 19–28 Aug. 1983* (Eds R Bergere, S Costa, C Schaerf) (Singapore: World Scientific, 1984) p. 412
11. Kazakov A A et al., in *Proc. of the II Intern. Seminar on Spin Phenomena in High Energy Physics, Serpukhov, 1985*, p. 140; in *Proc. of the IX Conf. of Charged Particles, Dubna, 1985*, Vol. 2, p. 268
12. Dowell D H et al., Prog. Rep. BNL 37623 (1985) p. 29
13. Bocquet J P et al., in *Proc. of the 13th Intern. Conf. on Particle and Nuclei* (*PANIC93*), *Perugia, Italy, 28 June–2 July 1993* (Ed. A Pascolini) (River Edge, NJ: World Scientific, 1994)
14. Ahn K et al., in *Proc. of the 12th Symp. on Accelerator Science and Technology, Wako, Japan, 1999* (Ed. Y Yano) (Wako: RIKEN, 1999) p. 141
15. Nedorezov V G, Gurevich G M, Kezerashvili G Ya, in *Physics and Chemistry of Fission*: *Proc. of the 18th Intern. Symp. on Nuclear Physics, Gaussig, DDR, 21–25 Nov. 1988* (Eds H Marten, D Seeliger) (New York: Nova Sci. Publ. Inc., 1992) p. 282
16. Ohgaki H et al. *IEEE Trans. Nucl. Sci.* **NS-38** 386 (1991)
17. Wu Y et al. *Nucl. Instrum. Meth. A* **375** 74 (1996)
18. Belyaev A D et al., in *Proc. of the X Intern. Seminar on Electromagnetic Interactions of Nuclei at Low and Medium Energies* (*EMIN-2003*), *Moscow, 16–18 April, 2003* (Ed. G M Gurevich) (in press)
19. Omelaenko A S et al., physics/9812001
20. Kazakov A A et al. *Pis'ma Zh. Eksp. Teor. Fiz.* **40** 445 (1984) [*JETP Lett.* **40** 1271 (1984)]
21. Ivanov D I et al. *Yad. Fiz.* **55** 3 (1992) [*Sov. J. Nucl. Phys.* **55** 1 (1992)]
22. Ivanov D I et al. *Yad. Fiz.* **55** 907, 2623 (1992) [*Sov. J. Nucl. Phys.* **55** 506, 1464 (1992)]
23. Ivanov D I et al. *Yad. Fiz.* **58** 1750 (1995) [*Phys. At. Nucl.* **58** 1650 (1995)]
24. Iljinov A S et al. *Nucl. Phys. A* **539** 263 (1992)
25. Akhmadaliev Sh Zh et al. *Phys. Rev. Lett.* **89** 061802 (2002)
26. Akhmadaliev Sh Zh et al., Preprint No. 99 (Novosibirsk: The Budker Institute of Nuclear Physics, Siberian Branch of the Russian Acad. of Sciences, 1998)
27. Sandorfi A M, in *Proc. of the 15th RCNP Intern. Symp. on Nuclear Physics Frontiers with Electroweak Probes* (*FRONTIER-96*), *Osaka, Japan, 7–9 March, 1996* (Eds H Toki, T Kishimoto, M Fujiwara) (Singapore: World Scientific, 1996) p. 17
28. Sandorfi A M et al. (LEGS Collab.), in *Excited Nucleons and Hadronic Structure*: *Proc. of the NSTAR 2000 Conf., Newport News, USA, 16–19 Feb. 2000* (Eds V D Burkert et al.) (Singapore: World Scientific, 2001) p. 22
29. Lowry M M et al., in *Testing QCD Through Spin Observables in Nuclear Targets*: *Workshop, Charlottesville, VA, USA, 18–20 Apr. 2002* (Eds D G Crabb, D B Day, J P Chen) (River Edge, NJ: World Scientific, 2003) p. 221
30. Bocquet J P et al. *Nucl. Phys. A* **622** c124 (1997)
31. Ajaka J, Anghinolfi M, Assafiri Y, in *3rd Latin American Workshop on Nuclear and Heavy Ion Physics, San Andrés, Colombia, 13–17 Sept., 1999*; *Acta Phys. Hung.*: *New Ser. Heavy Ion Phys.* **11** 421 (2000)
32. Bartalini O et al. (GRAAL Collab.), in *ICTP 3rd Intern. Conf. on Perspectives in Hadronic Physics, Trieste, Italy, 7–11, 2001*; *Nucl. Phys. A* **699** 218 (2002)
33. Nakano T et al. *Nucl. Phys. A* **684** 71 (2001)
34. Fujiwara M et al. *Acta Phys. Pol. B* **29** 141 (1998)
35. Fujiwara M *Prog. Part. Nucl. Phys.* **50** 487 (2003)
36. Aritomo Y et al., in *Proc. of the Intern. Workshop on Laser Electron Photons at Spring-8* (*LEPS 2000*), *Garden City, Japan, Oct. 14–15, 2000* (Eds M Yosoi, H Shimizu) (Osaka: Res. Center for Nucl. Phys., Osaka Univ., 2001)
37. Ahrens J *Nucl. Phys. A* **446** 229 (1985)
38. Golubeva Ye S et al. *Eur. Phys. J. A* **11** 237 (2001); nucl-th/0103082
39. Zavarzina V P, Stepanov A V *Kratk. Soobshch. Fiz.* (9) 43 (1998) [*Bull. Lebedev Phys. Inst.* (9) 36 (1998)]
40. Ries H et al. *Phys. Lett. B* **139** 254 (1984)
41. Bianchi N et al. *Phys. Rev. C* **54** 1688 (1996)
42. Vinogradov Yu A et al. *Yad. Fiz.* **24** 686 (1976) [*Sov. J. Nucl. Phys.* **24** 357 (1976)]
43. Sanabria J C et al. *Phys. Rev. C* **61** 034604 (2000)
44. Cetina C et al. *Phys. Rev. C* **65** 044622 (2002)
45. Pshenichnov I A et al., nucl-th/0303070
46. Armstrong T A et al. *Phys. Rev. D* **5** 1640 (1972)
47. Armstrong T A et al. *Nucl. Phys. B* **41** 445 (1972)
48. MacCormick M et al. *Phys. Rev. C* **55** 1033 (1997)
49. Bianchi N et al. *Phys. Rev. C* **60** 064617 (1999)
50. Muccifora V et al. *Phys. Rev. C* **60** 064616 (1999)
51. Levinger J S *Phys. Lett. B* **82** 181 (1979)

52. Rudnev N V et al., in *Proc. of the X Intern. Seminar on Electromagnetic Interactions of Nuclei at Low and Medium Energies* (*EMIN-2003*), *Moscow, 16 – 18 April, 2003* (Ed. G M Gurevich) (in press)
53. Aleksandrov B M et al. *Yad. Fiz.* **43B** 290 (1986)
54. Ivanov D I et al. *Nucl. Phys. A* **485** 668 (1988)
55. Mebel' M V, private communication
56. d'Hose N, in *Trudy IX Seminara* "*Elektromagnitnoe Vzaimodeĭstvie Yader pri Malykh i Srednikh Energiyakh*" (Proc. of the IX Seminar "Electromagnetic Interactions of Nuclei at Low and Intermediate Energies") (Moscow: Izd. IYaI RAN, 2003) p. 223
57. Korchin A Yu, Scholten O *Nucl. Phys. A* **684** 426 (2001)
58. Polikanov S et al. *Z. Phys. A* **350** 221 (1994)
59. Aumann T et al. *Phys. Rev. C* **47** 1728 (1993)
60. Belyaev S T et al., Preprint No. 5046/2 (Moscow: IAE, 1990)
61. Milstein A I, Schumacher M *Phys. Rep.* **243** 183 (1994)
62. Milshtein A I, in *Proc. of the 3rd Intern. Seminar on High Energy Physics and Thermonuclear Research, Novosibirsk, Russia, 11 – 15 May, 1998* (Novosibirsk: BINP, 1998) p. 161
63. Milshtein A I, Strakhovenko V M *Phys. Lett. A* **95** 135 (1983)
64. Federichi L et al. *Nuovo Cimento B* **59** 247 (1980)
65. Thorn C E et al. *Nucl. Instrum. Meth. A* **285** 447 (1989)
66. Steven C et al. (LEGS Collab.), in *Proc. of the Intern. Workshop on Laser Electron Photons at Spring-8* (*LEPS 2000*), *Garden City, Japan, Oct. 14 – 15, 2000* (Eds M Yosoi, H Shimizu) (Osaka: Res. Center for Nucl. Phys., Osaka Univ., 2001)
67. Molinari C et al. *Phys. Lett. B* **371** 181 (1996)
68. Hallin E L et al. *Phys. Rev. C* **48** 1497 (1993)
69. Genzel H et al. *Z. Phys. A* **279** 399 (1976)
70. Barbiellini G et al. *Phys. Rev.* **174** 1665 (1968)
71. Genzel H et al. *Z. Phys. A* **268** 43 (1974)
72. Ganenko V B et al. *Yad. Fiz.* **23** 310 (1976) [*Sov. J. Nucl. Phys.* **23** 162 (1976)]
73. Anghinolfi M et al., in *Proc. of the 13th Intern. Conf. on Particle and Nuclei* (*PANIC93*), *Perugia, Italy, 28 June – 2 July 1993* (Ed. A Pascolini) (River Edge, NJ: World Scientific, 1994) p. 785
74. Girolami B et al., in *Proc. of the 6th Intern. Conf. on Calorimetry in High Energy Physics* (*ICCHEP96*), *Rome, Italy, June 8 – 14, 1996* (Frascati Phys. Ser., Vol. VI, Ed. A Antonelli) (Frascati: LNF, 1996) p. 727
75. Kouznetsov V et al. *Nucl. Instrum. Meth. A* **487** 396 (2002)
76. Bussey P J et al. *Nucl. Phys. B* **154** 205 (1979)
77. Zdarko R, Dolly E *Nuovo Cimento A* **10** 10 (1972)
78. Knies G et al. *Phys. Rev. D* **10** 2778 (1974)
79. SAID, http://said.phys.vt.edu
80. Drechsel D et al. *Nucl. Phys. A* **645** 145 (1999)
81. Bartalini O et al. (GRAAL Collab., GW-SAID Group) *Phys. Lett. B* **544** 113 (2002)
82. Krusche B et al. *Phys. Rev. Lett.* **74** 3736 (1995)
83. Bennhold C et al., nucl-th/9901066; nucl-th/0008024
84. Nedorezov V, Unformal Report for GRAAL Collab. (2002) (not published)
85. Nakano T et al. (LEPS Collab.) *Phys. Rev. Lett.* **91** 012002 (2003); hep-ex /0301020
86. Nedorezov V G, in *Proc. of the IX Seminar EMIN 2000, Moscow,* (Ed. G M Gurevich) (Moscow: INR, 2000) p. 170
87. Utsonomia H et al., in *Proc. of the Intern. Conf. LEP 2001* (Osaka: USP Publ., 2001) p. 83
88. Baĭer V N, Khoze V A *At. Energ.* **25** 440 (1968)
89. Gustavson D B et al. *Nucl. Instrum. Methods* **165** 177 (1979)
90. Vorob'ev P V et al., in *Trudy VIII Vsesoyuz. Soveshch. po Uskoritelyam Zaryazhennykh Chastits, Dubna* (Proc. of the VIII All-Union Workshop on Charged Particle Accelerators, Dubna) Vol. 2 (Editor-in-Chief A A Vasil'ev) (Dubna: OIYaI, 1982) p. 272
91. Barber D P et al. *Phys. Lett. B* **343** 436 (1995)
92. Assmann R et al. *Z. Phys. C* **66** 567 (1995)
93. Shintake T et al., in *Proc. of the 15th Intern. Conf. on High Energy Accelerators, Hamburg, Germany, Jily 20 – 24, 1992*; *Int. J. Mod. Phys. A Proc. Suppl.* **2A** 215 (1993)
94. Kezerashvili G Ya, Skrinsky A N, in *Proc. of the Workshop on Advanced Beam Instrumentation, Tsukuba, Japan, 22 – 24 April 1991* Vol. 1 (Eds A Ogata, J Kishiro) (Tsukuba: KEK, 1991) p. 183
95. Kremyanskaya E V et al., in *Trudy 2-ĭ Baĭkal'skoĭ Shkoly po Fundamental'noĭ Fizike* (Proc. of the 2nd Baikal School in Fundamental Physics) (Ed. Yu N Denisyuk) (Irkutsk: Izd. Irkutskogo Univ., 1999)